DNMI

DMI DNMI SMHI

NORDKLIM – Nordic co-operation within Climate activities

Nordic temperature maps

O.E.Tveito, E.Førland, R.Heino, I.Hanssen-Bauer
H.Alexandersson, B.Dahlström, A.Drebs, C.Kern-Hansen
T.Jónsson, E. Vaarby Laursen, Y.Westman

Report no. 09/00

KLIMA

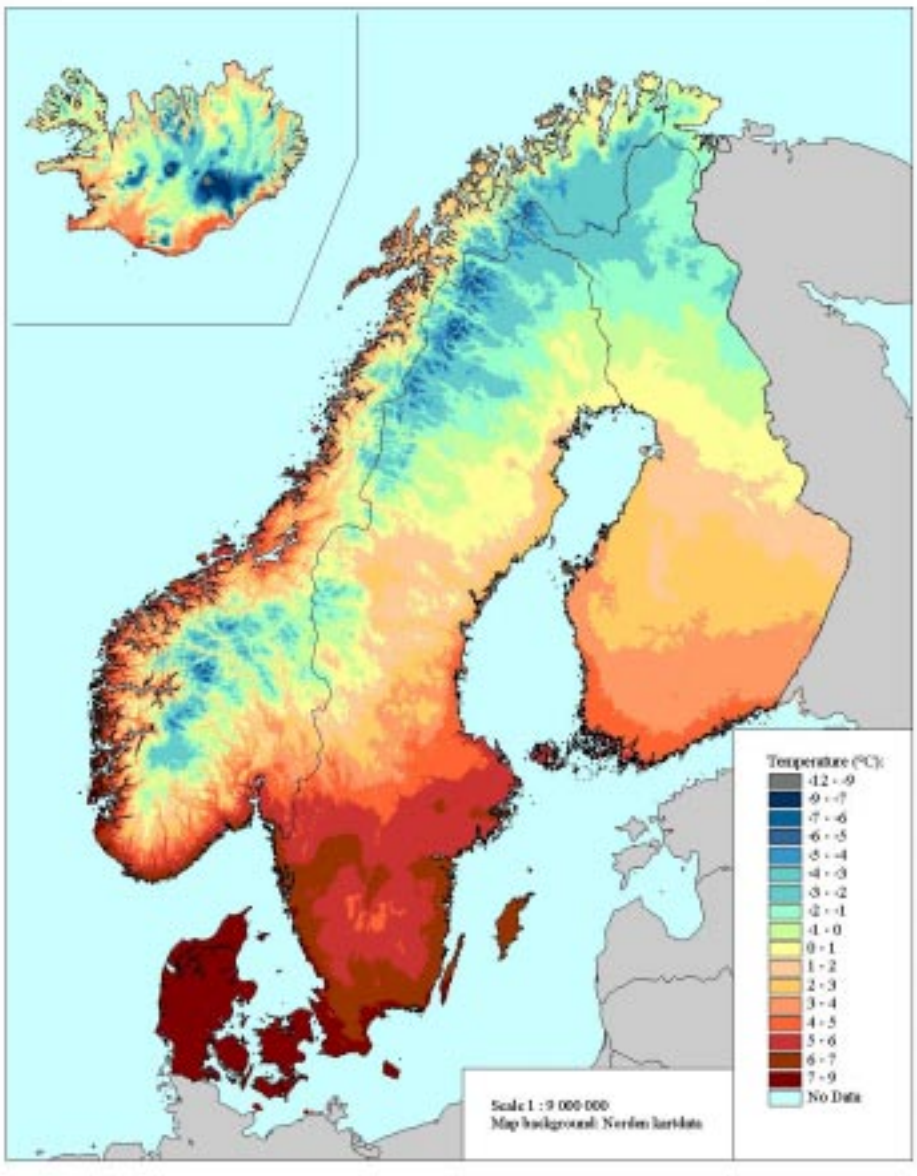

DNMI - REPORT

ISSN 0805-9918

NORWEGIAN METEOROLOGICAL INSTITUTE
BOX 43 BLINDERN , N - 0313 OSLO, NORWAY

PHONE +47 22 96 30 00

REPORT NO.
09/00 KLIMA
Revised edition

DATE
17.11.00

TITLE:

Nordic temperature maps

AUTHORS:

O.E.Tveito[N], E.Førland[N], R.Heino[F], I.Hanssen-Bauer[N], H. Alexandersson[S], B.Dahlström[S], A.Drebs[F], C.Kern-Hansen[D], T.Jónsson[I], E. Vaarby Laursen[D], Y.Westman[S]

[D)] DMI Denmark, [F)] FMI Finland, [I)] VI Iceland, [N)] DNMI Norway, [S)] SMHI Sweden

PROJECT CONTRACTORS:

NORDKLIM/NORDMET on behalf of the National meteorological services in Denmark (DMI), Finland (FMI), Iceland (VI), Norway (DNMI) and Sweden (SMHI)

SUMMARY:

This report is prepared under Task 2 in the Nordic NORDKLIM project: Nordic Co-Operation Within Climate Activities. The NORDKLIM project is a part of the formalised collaboration between the NORDic METerological institutes, NORDMET.

This report presents the first monthly, seasonal and annual temperature maps for the period 1961-90 covering the entire Nordic region. The maps are derived by applying an objective interpolation technique (residual kriging), combined with the utilization of a geographical information system (GIS). The interpolation method involves a trend expression, which was established by linear regression analysis. Different elevation models and geographical location were applied as independent variables. Different models were established for Fennoscandia and Iceland. The temperature maps derived by applying this interpolation method shows to be reliable.

KEYWORDS:

Temperature, Geographical information systems (GIS), linear regression, residual kriging

SIGNATURES:

.....	.....
Eirik J. Førland	Bjørn Aune
NORDKLIM Activity Manager	Head of the DNMI Climatology Division

Foreword

This report is prepared under task 2 in the Nordic NORDKLIM project: *Nordic Co-Operation Within Climate Activities.* The NORDKLIM project is a part of the formalised collaboration between the NORDic METeorological institutes, NORDMET.

The main objectives of NORDKLIM are:
1). Strengthening the Nordic climate competence for coping with increased national and international competition
*2). Improving the cost-efficiency of the Nordic meteorological services (i.e. by i*mproving procedures for standardized quality control & more rational production of standard climate statistics)
3). Coordinating joint Nordic activities on climate analyses and studies on long-term climate variations

The NORDKLIM project has two main tasks:

1. Climate data (Network design, Quality control, Operational precipitation correction, long-term datasets).

2. Climate Applications (Time series analysis, use of GIS within climate applications, mesoscale climatological analysis).

A detailed description of the project is given by Førland et al.(1998).

NORDKLIM is coordinated by an Advisory Committee, headed by an Activity Manager. Each of the main tasks is headed by a Task manager.

The Advisory Committee in NORDKLIM is presently consisting of:

Bengt Dahlström, SMHI
Eirik J. Førland, DNMI (**Activity Manager**)
Raino Heino, FMI
Trausti Jónsson, VI
Lillian Wester Andersen, DMI

The present task managers are: Task 1: Pauli Rissanen (FMI), Task 2: Ole Einar Tveito (DNMI)

The addresses of the Nordic Meteorological Institutes are:
Denmark: Danish Meteorological Institute, Lyngbyvej 100, DK-2100 Copenhagen, Denmark, (www.dmi.dk)
Finland: Finnish Meteorological Institute, P.O.B.503, FIN-00101 Helsinki, Finland, (www.fmi.fi)
Iceland: Vedurstofa Islánds, Bustadavegur 9, IS-150 Reykjavik, Iceland, (www.vedur.is)
Norway: Norwegian Meteorological Institute, P.O.Box 43 Blindern, N-0313 Oslo, Norway, (www.dnmi.no)
Sweden: Swedish Meteorological and Hydrological Institute, S-60176 Norrköping, Sweden, (www.smhi.se)

Contents

Introduction

For some of the Nordic countries, national maps of the standard normal monthly and annual temperatures during the period 1961-90 have been published, e.g. for Norway (Aune, 1993) and Sweden (Raab & Vedin, 1995). For Finland Alalammi (1987) have presented maps referring to the period 1931-60. Different techniques and resolutions are used for these national maps, and consequently they are difficult to compare. The objective mapping technique applied in this report represents a uniform, consistent analysis over the whole region.

Table 1: Number of stations from each country

Country	No. of stations
Denmark	44
Finland	167
Iceland	95
Norway	421
Sweden	520

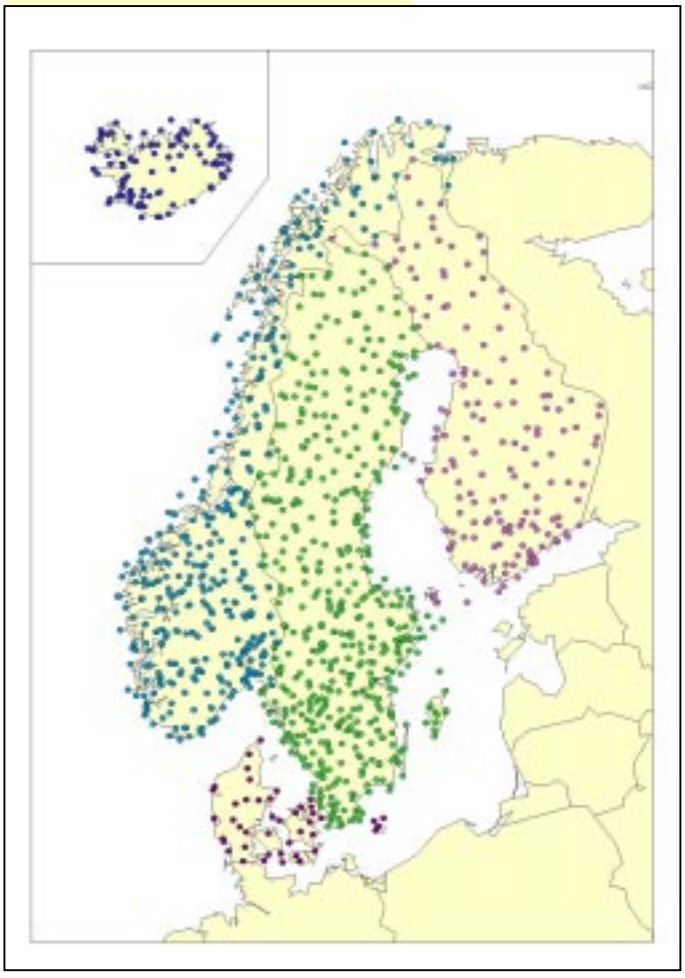

Figure 1: Temperature stations in Fennoscandia used in the analysis

The standard normals for the period 1961-90 are calculated at the national meteorological institutes. Normals are defined by the World Meteorological Organisation (WMO, 1989) as: *"period averages computed for a uniform and relatively long period comprising at least three consecutive ten-years periods"*. Climatological standard normals are defined as "averages of climatological data computed for consecutive periods of 30 years as follows: 1901-1930, 1931-1960, 1961-1990 etc". In the case of series where some data are missing, provisional normals are calculated, based on comparisons with neighbouring stations with complete records. In this report "normal" is used synonymous with "*climatological standard normals*".

When the International Meteorological Organization in 1935 agreed to calculate "normals", one requirement was that the length of the normal period should be sufficient to reflect climatic changes. Too long periods might prove insensitive to real climatic trends, whereas too short periods would be over-sensitive to random climatic variations. It was feared that the 11-years sunspot periods might influence climatic variations. For these reasons it was decided to operate with an averaging period of 30 years. However, e.g. Hanssen-Bauer et al. (1996) have stated that over Northern Europe there are large decadal variations, influencing even 30-years averaging periods (see also Førland et al., 1996). In addition there are also significant long-term temperature trends in parts of the Nordic region. This is highlighted in the last section of this report.

In this study monthly standard normal temperatures from 1247 stations are applied in the analysis. The locations of the stations are shown in figure 1. Table 1 shows the number of stations available from each country.

The station cover is good in southern parts of Sweden and Finland and south-eastern Norway. The station network is sparse in the mountains, northern parts and in western Jutland (Denmark).

The spatial analysis, methods and results.

The analysis applies residual kriging (Tveito and Førland, 1999), also referred to as detrended kriging (Prudhomme and Reed, 1999). Measured temperatures are a result of physical processes in the atmosphere, influenced by local effects. The method used in this analysis is based on the principle that temperature can be described as a sum of deterministic and stochastic processes. The large-scale trend (deterministic components) can be found by analysing digital maps of e.g. topography. Temperature is related to altitude by the vertical lapse rate. In dry air, the atmosphere is neutrally stratified when the lapse rate is 9.8°C/km. When the atmosphere is saturated, rising air will cool more slowly than 9.8°C/km because of the release of latent heat of condensation. The rate is lowest for warm air and approaches the dry adiabatic lapse rate for very cold air. Typically, the moist adiabatic lapse rate is about 6.5°C/km and closely matches the average observed lapse rate in the troposphere (Houghton, 1985). During special weather situations, the lapse rate may deviate substantially from these average conditions. During inversion situations, the temperature in the lower troposphere may even increase by increasing altitude.

The deterministic components describe features that are global for the entire study area. The local variability is described by spatial statistics applied on the residuals obtained by removing the global trend.

Finding the trend components.
In this study, linear regression has been used for defining the trend terms. Since the influence of the different variables is of interest, stepwise regression has been applied.

Based on the results obtained by Tveito and Førland (1999), five independent variables are chosen to describe the large-scale spatial climate trends. Three of these are based on topography, the two last are longitude and latitude, which in combination describes both distance to sea and latitudinal variability.

The vertical temperature gradient is by many authors regarded as the most dominating trend component, often defined as the standard lapse rate of -6.5°C/km. Studies by Bruun (1957) and Tveito and Førland (1999) have however showed that this lapse rate varies with the season. Bruun (1957) showed in her work that this variation also depends on the local terrain characteristics. The work by Tveito and Førland (1999) revealed that despite giving a good description, station altitude does not give sufficient explanation of the spatial variability of

temperature, especially during the winter season. Therefore two other topographical parameters are defined. The mean altitude within a 20 km radius around the station, as well as the minimum altitude within the same circle both gives an indirect measure of the local terrain at the station relative to the meso-scale terrain. The idea is that stations at high levels (e.g. hill tops) compared the surroundings show other features than stations located in lower levels (e.g. kettles). Since linear expressions are used, any linear combinations of these three features are accounted for. The terrain model applied is the GTOPO30 digital elevation model (USGS, 1996), which was resampled to a basic resolution 1 x 1 km^2.

Oceans act as a heat conservator, which influence the temperature conditions. The wind conditions near the oceans are also different from more protected areas in continental areas. Therefore distance to sea is a parameter that can explain spatial variability of temperature (Førland, 1984, Zheng & Basher, 1996). In this study longitude is used to explain the continentality.

Since Fennoscandia (Denmark, Finland, Norway and Sweden) and Iceland are projected to different conditions, different trends are defined for the two regions.

Trend components for Fennoscandia.

Regression expressions for each month are established by linear stepwise regression using the five parameters described above as independent variables. The reason for using stepwise regression was that the level of entry, and how it varies throughout the year, for each variable is of interest discussing the individual contribution from the variables. Figure 2 shows the gridded maps of these five independent variables.

The resulting trend equations[1] cover between 84 and 97 % of the variance for all months. Table 2 shows the results of the analysis, with the regression coefficients for all variables, entry level, coefficient of determination when all variables are entered and standard error. Figure 3 shows the seasonal variation of the regression coefficients. Correlation coefficients between the monthly mean temperatures and the independent variables are shown in figure 4.

[1] In the data sets used in this analysis, altitude is noted in meters. When discussing the results the relation between temperature and altitude, it will be in °C/m, and not as °C/km as earlier in this document. (6.5°C/km=0.0065°C/m).

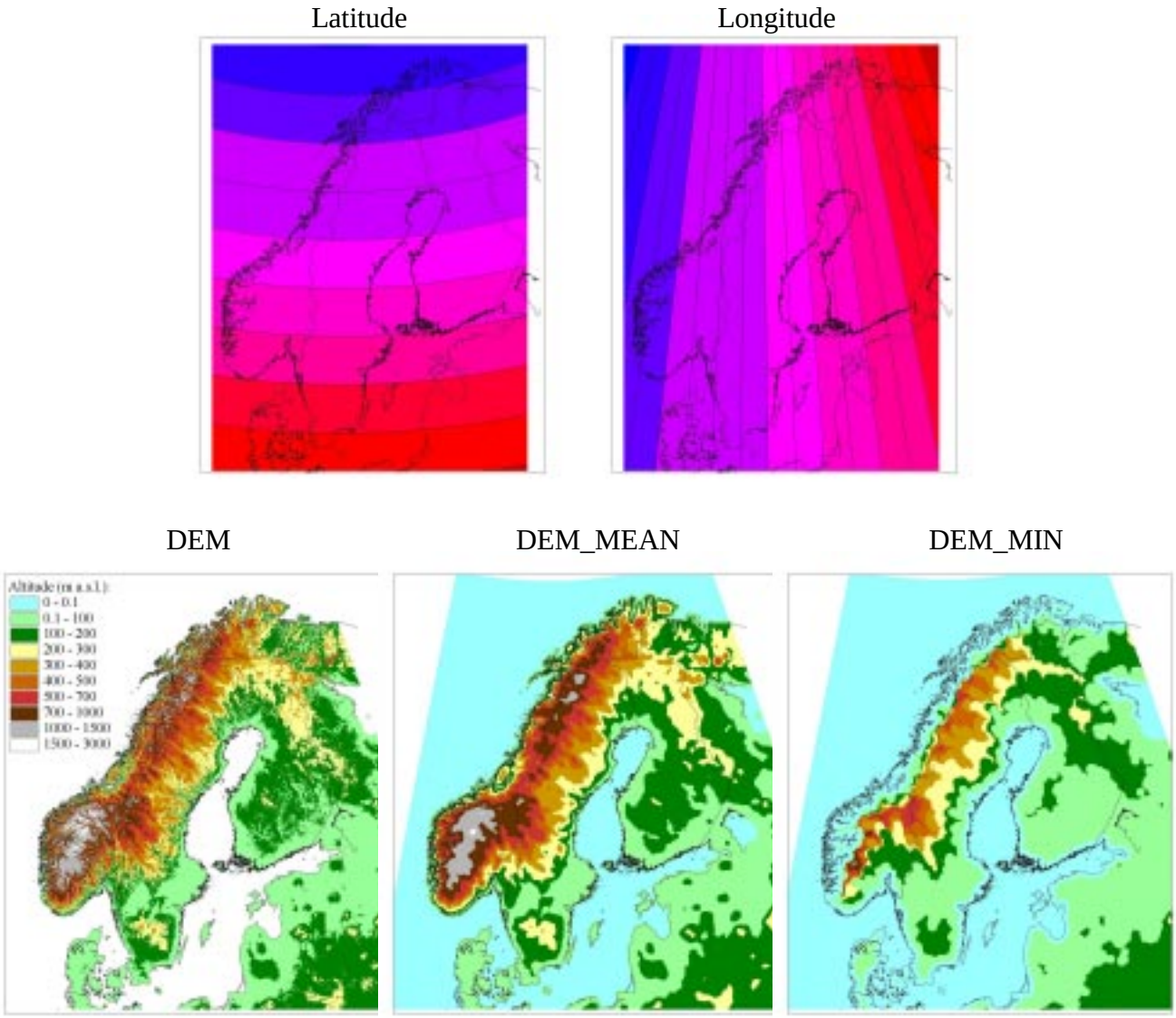

Figure 2: Gridded maps of the parameters used as independent variables used for establishing the trend expressions.

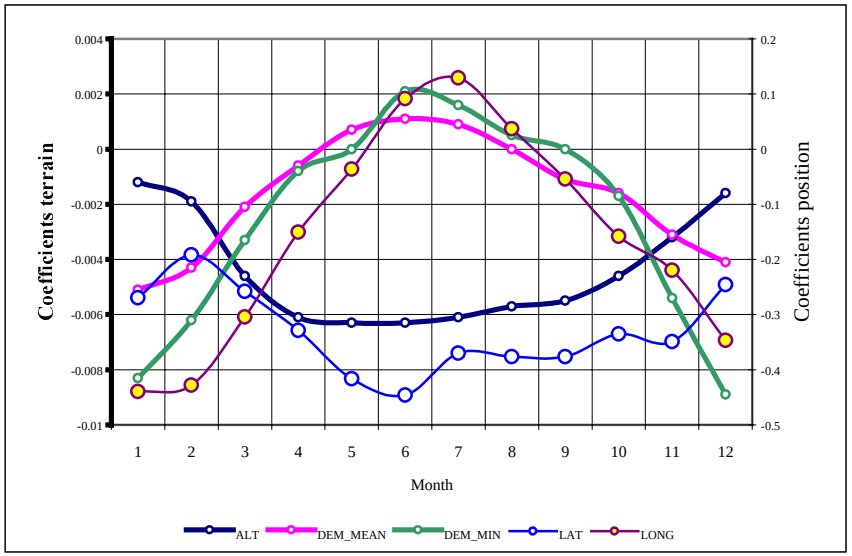

Figure 3: Monthly variability of the regression coefficients for Fennoscandia

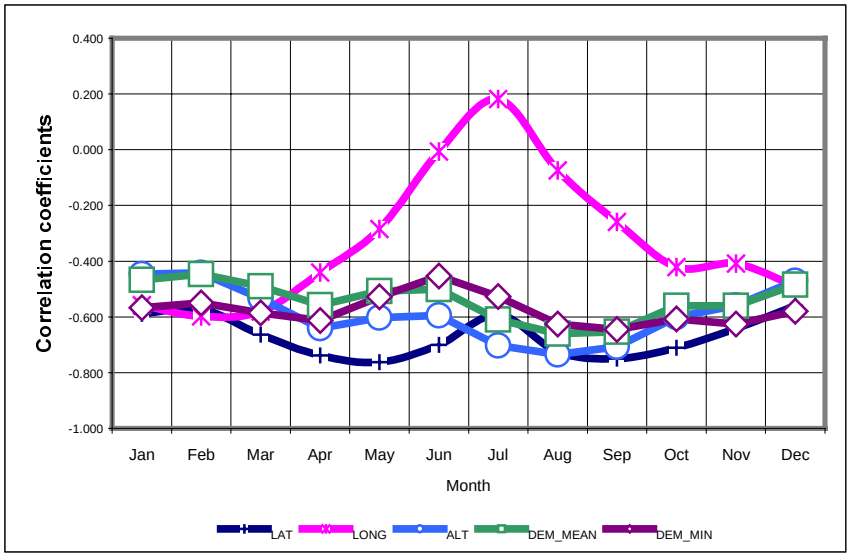

Figure 4: Monthly variability of the correlation coefficients for Fennoscandia

Table 2: Linear regression estimating deterministic trends in Fennoscandian temperature normals:

ALT:	Station altitude
DEM_MEAN:	Mean altitude calculated from a DEM in a 20 km circle around the gridcell containing the station.
DEM_Min:	Minimum altitude in the DEM with in a 20 km circle around the gridcell containing the station.
LAT:	Latitude (decimal degrees) of the station
LONG:	Longitude of the station.

MONTH	JAN		FEB		MAR		APR		MAY		JUN		JUL		AUG		SEP		OCT		NOV		DEC	
ALT	5	-0.0012	5	-0.0019	4	-0.0046	2	-0.0061	2	-0.0063	2	-0.0063	1	-0.0061	1	-0.0057	2	-0.0055	2	-0.0046	5	-0.0032	5	-0.0016
DEM_MEAN	4	-0.0051	2	-0.0043	5	-0.0021	4	-0.0006	4	0.0007	5	0.0011	5	0.0009	-	-	4	-0.0011	4	-0.0016	4	-0.0031	3	-0.0041
DEM_MIN	2	-0.0083	4	-0.0062	2	-0.0033	5	-0.0008	-	-	4	0.0021	4	0.0016	4	0.0005	-	-	5	-0.0017	2	-0.0054	1	-0.0089
LAT	1	-0.2694	3	-0.1918	1	-0.2579	1	-0.3288	1	-0.4166	1	-0.4460	2	-0.3700	2	-0.3763	1	-0.3764	1	-0.3349	1	-0.3491	4	-0.2459
LONG	3	-0.4395	1	-0.4282	3	-0.3044	3	-0.1505	3	-0.0363	3	0.0914	3	0.1290	3	0.0370	3	-0.0543	3	-0.1581	3	-0.2194	2	-0.3470
(Constant)		19.4879		14.7045		19.8752		26.0346		35.1963		39.4180		35.9240		36.8990		34.4318		29.1849		25.9764		18.0301
R^2		0.88		0.89		0.94		0.97		0.92		0.89		0.93		0.98		0.98		0.93		0.88		0.84
R square		0.77		0.79		0.89		0.94		0.85		0.81		0.87		0.95		0.95		0.86		0.77		0.70
S.E.		2.21		1.86		1.07		0.64		0.94		0.96		0.71		0.45		0.52		1.04		1.72		2.26

The correlation coefficient shows the dependencies between the mean monthly temperature and the variables we are using to describe the trend component. These dependencies are not constant throughout the year, and different variables will have different importance in different seasons. The most dramatic variation is seen for longitude. This is the variable that (indirectly) explains the large-scale continentality in this region. Continentality is in reality described as distance from the Atlantic Ocean, neglecting the Baltic Sea. In a large-scale consideration this is acceptable, since the influence of the Baltic Sea will be accounted for in other variables, or in the residual kriging.

The latitudinal signal is reflecting the north-south gradient, i.e. the incoming radiation. The correlation is poorest during winter and summer. This is caused by large gradients between coastal and continental areas. The reason may be that during high pressure situations, high temperatures may occur during summer, and very low temperatures in winter time in continental areas. In coastal areas, temperature variability is lower since the heat conservating properties of the ocean damp the temperature variability.

The terrain parameters show different correlations during the year. In wintertime, the regional altitude measures (DEM_MEAN and DEM_MIN) have the highest correlation, while the station altitude (ALT) shows higher correlations between April and September. In the winter months, local terrain conditions may cause large local gradients, e.g. occurrence of inversions. Consequently the station altitude has less influence in the winter season, where the coefficient is as low as −0.0012 °C/m. The influence increases until April where the coefficient reach levels below −0.006 °C/m, close to the standard lapse rate. The influence decreases again during the autumn. These results support the indications found by studying the correlation coefficients that local variability of temperature is difficult to explain by only at-site altitude during winter period. Also Machenhauer et al. (1998) found a marked seasonal variation in the lapse rate over Europe, applying the CRU-dataset. They found however little geographical variation in the lapse rate over Europe. Even Machenhauer et al. (op.cit.) found that all monthly values were lower than the standard lapse (°C/km) (J=5.01, F= 5.66, M=6.01, A= 5.97, M= 5.88, J=5.84, J=5.53, A=5.22, S=5.33, O=5.24, N=5.21, D=4.94)

The regression coefficients of the two terrain parameters describing the regional terrain show an opposite contribution to the trend component than the station altitude. The contribution is high in winter, and especially DEM_MIN is important. This parameter has no significant influence in summertime, and act as an indicator for inversions. The idea is that the distance between DEM_MIN and ALT (and also DEM_MEAN and ALT) will reveal systematic relations for station located low or high related to the regional terrain. These relations are expressed as the linear combination of these three parameters. It seems that DEM_MEAN and DEM_MIN explain much of the same features. It is worth to notice that they are contributing instead of ALT and vice versa.

Stochastic interpolation.
The stochastic component accounts for the variations not described by the trend components. This component varies on a local scale, and it is assumed that it can be described by a spatial co-variance function. In this analysis kriging (Cressie, 1991) is used as interpolation method. Thus semivariogram is used to describe the spatial covariance. For other purposes, the co-variance function can be used directly, as in the MESAN system (Foltescu & Foltescu, 2000).

Table 3: Semivariogram parameters

Month	Nugget	Sill	Range (km)	
Jan	0.00092	7.0	250	*
Feb	0.00122	5.0	250	*
Mar	0.00062	1.3	200	*
Apr	0.10000	0.33	100	*
May	0.00027	0.7	75	*
Jun	0.00036	1.0	150	*
Jul	0.09000	0.6	500	**
Aug	0.07500	0.19	100	*
Sep	0.08000	0.3	75	*
Oct	0.00030	1.3	175	*
Nov	0.00033	3.5	200	*
Dec	0.00032	7.0	250	*

*) Exponential model applied
**) Spherical model applied

Semivariograms for detrended temperatures are established for each month, and both spherical and exponential semivariogram models were fitted to the experimental semivariogram. The exponential model was used for all months except July. Table 3 shows the parameters used in the selected models. Figure 5 shows semivariograms for some months (January, April, July and November).

Kriging is used to interpolate the residual fields with grid resolution of 5×5 km^2. The trend components are added to this field, and these have 1×1 km^2 resolution, which also is the resolution of the final maps. 5×5 km^2 kriging resolution is chosen in order to reduce the calculation time. The number of cells to estimate is reduced 25 times compared to 1×1 km^2 grid size, and the assumption is that the residual temperature fields are so smooth that details are not lost by applying larger grid cells.

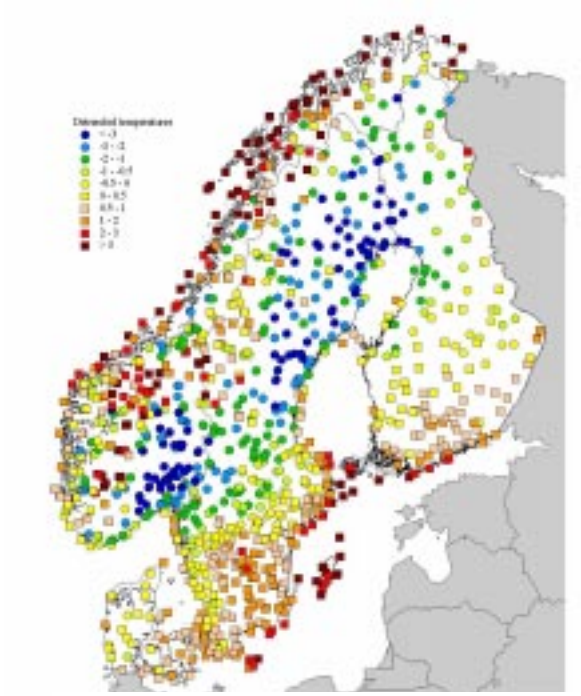

Figure 6a Detrended temperatures for January

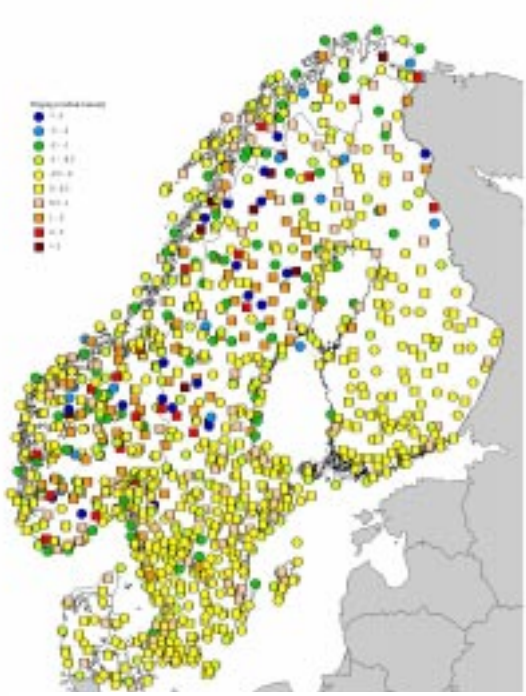

Figure 6b Crossvalidation results for January

Verification

The results of the kriging-interpolation are verified by cross-validation. This means that the temperature at each station is estimated based on observations from all the other stations. Maps showing the residual temperatures and the difference between observed and estimated station temperatures for some typical months (January, April, July and November) are presented.

Figure 6b shows cross validation results for January. The map indicates the goodness of the interpolation of the temperature residuals (Figure 6a). It can be seen that the estimates are poor in the inland, especially in Norway and northern parts of Sweden. The temperature residuals (figure 6a) show systematic patterns. There are distinct gradients oriented in a north-eastern direction. The sharp gradient results in poor estimates in inland, and this effect is also enhanced due to a mixture of stations in higher altitude levels and valley stations. Temperatures in valleys are during winter often lower than in the surrounding mountains because of inversions. Therefore more terrain parameters than just station altitude are included in the trend components. The present cross-validation map shows better estimates than similar maps for a smaller and more homogenous region (southern Norway) presented by Tveito and Førland (1999), which only applied station altitude in the trend expression.

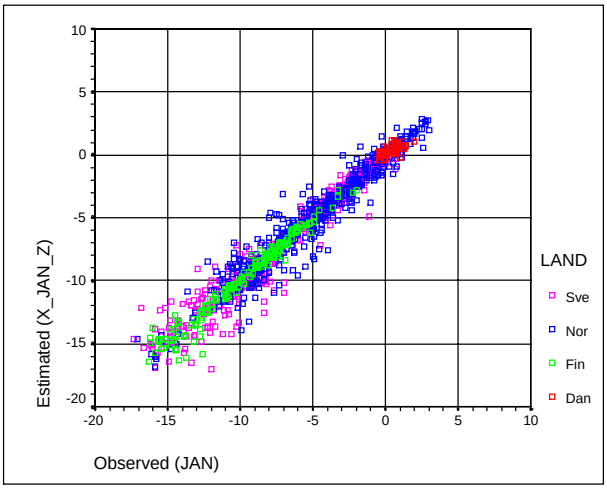

Figure 7a Observed vs. estimated temperatures in January

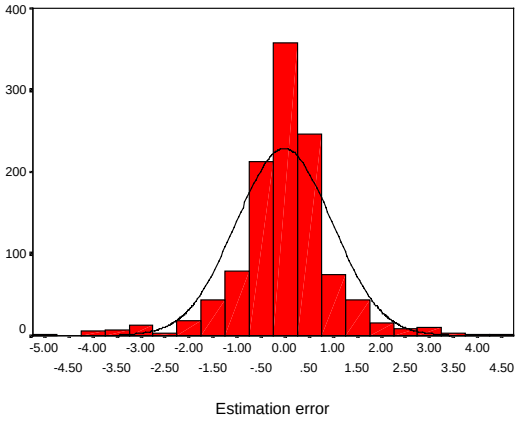

Figure 7b Frequency distribution of estimation errors in January

Considering the goodness of the temperature estimates at station level, the estimates are compared with the observations. Figure 7a shows the scatter between observations and estimates. January is characterised by a very large temperature range within the region. It spans from -17 to +3°C. Most of the stations have estimates close to the diagonal. Figure 7b shows that the distribution of errors follow the normal distribution, and most of the errors are within ±1.5 °C.

The uncertainties in the January temperature estimates can be explained by two climatological features. In the winter season inversions occur frequently, especially in continental parts. In addition the temperature gradients are large. Both these factors are partly covered by the trend expression. However, the station cover is biased, with a much denser network in the southern parts. Since this area is relatively homogenous considering temperature and topography, the conditions in this area will be given high attention in the regression analysis defining the trend expression. Other areas do not have the same homogenous features, and is thereby

suppressed in the same regression analysis.

Examination of the April temperature estimates shows much smaller errors than for January. The conditions in the spring is much more homogenous than in the winter. Both the crossvalidation map (figure 8b) and the map of residual temperatures (Figure 8a) show very little variation. This means that the trend expression describes the conditions well. At station level the scatterplot (Figure 9a) reflects this. It shows that the points are tightly clustered around the diagonal. Figure 9b shows the frequencies of estimation error at station level, and all stations have errors less than ±1.7°C. Very few stations (30 of 1152 = 2.6%) have errors larger than ±1°C.

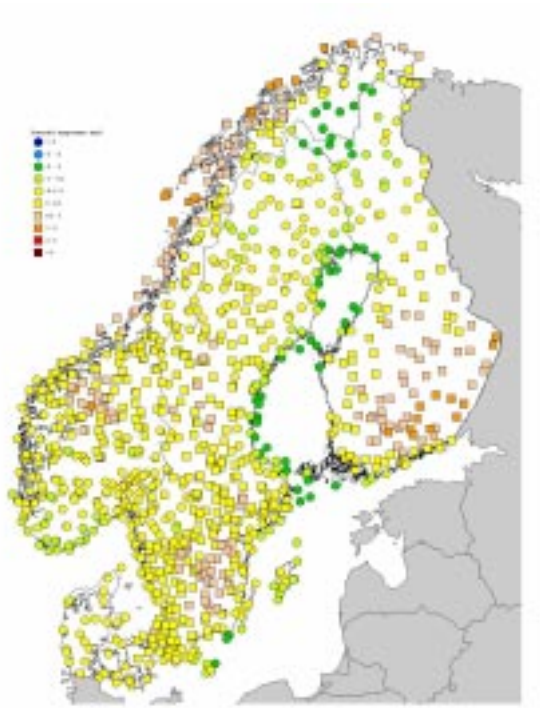

Figur 8a Detrended temperatures April

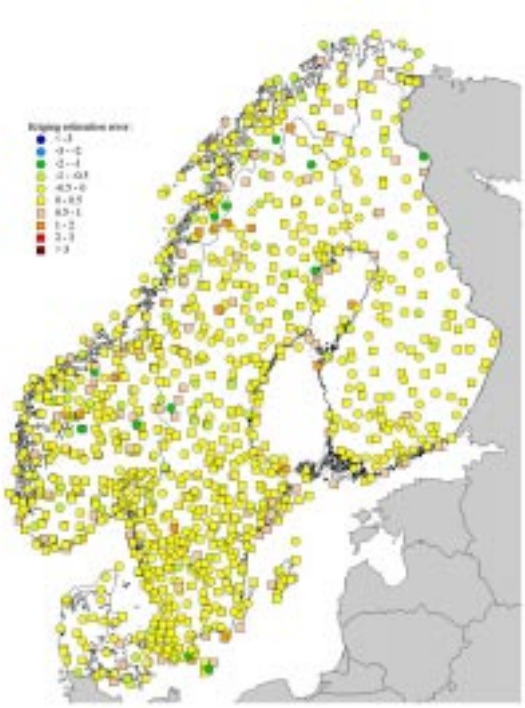

Figure 8b Crossvalidation results, April

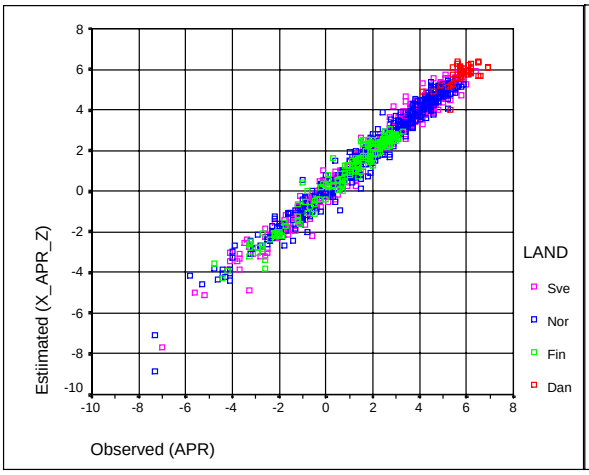

Figure 9a Observed vs. estimated temperatures April

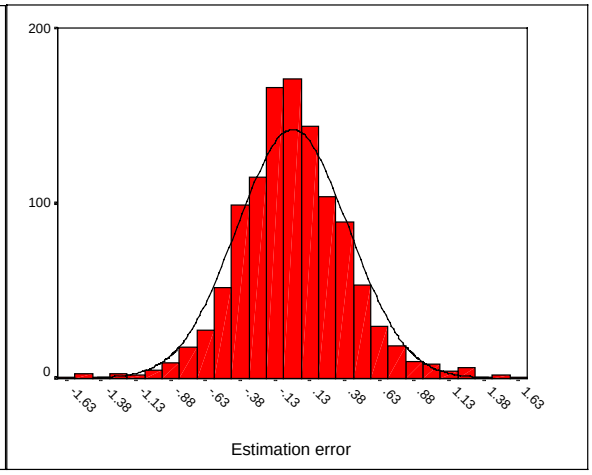

Figure 9b Frequency distribution of estimation errors in April

July is selected as example for the summer season, and the crossvalidation results (figure 10b) shows good fit. Just a few single stations have errors larger than 1°C. These stations are randomly located. Also the map of temperature residuals (Figure 10a) shows regional patterns. The detrended temperatures around the Oslo-fjord are warmer than the surrounding areas. On the other hand there are negative temperature residuals at the western coast of Norway, southern coast of Sweden and northern Norway.

For the lowest temperatures in July, figure 11a shows that they are estimated too high. The frequency plot (Figure 11b) shows that most estimates are good, and that there are a few large positive errors.

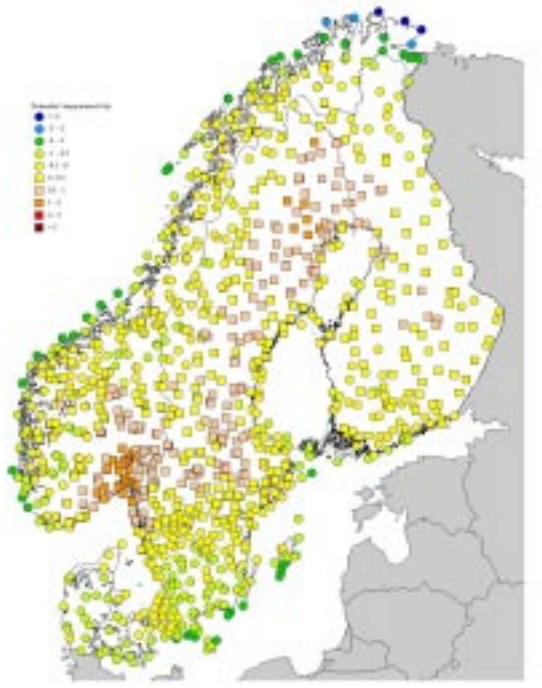

Figure 10a Detrended temperatures for July

Figure 10b Crossvalidation results July.

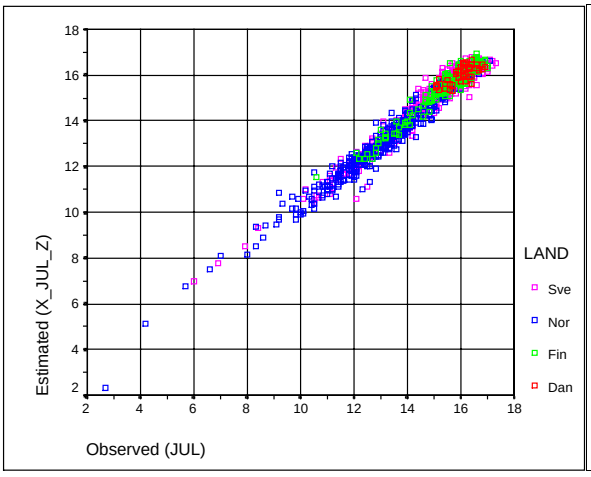

Fgure 11a Observed vs. estimated temperature July

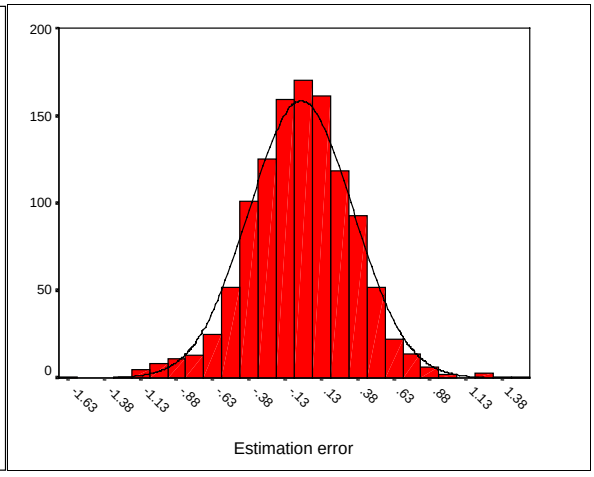

Figure 11b Frequency of estimation errors July.

The detrended temperatures in November are in many ways similar to January (Fig 12a). Large estimation errors are found in the mountain areas of Sweden and Norway (Fig 12b). The kriging estimation errors are normally distributed, and most of the errors are within 1° C (Fig 13b).

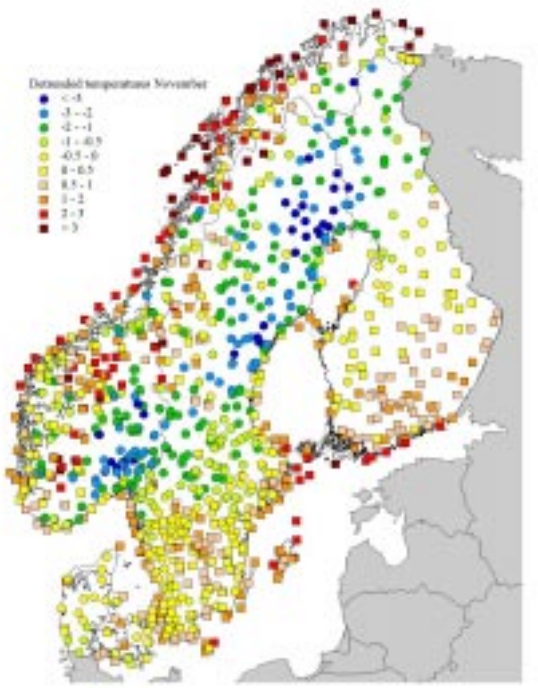

Figure 12a Detrended temperatures, November.

Figure 12b Kriging estimation errors, November.

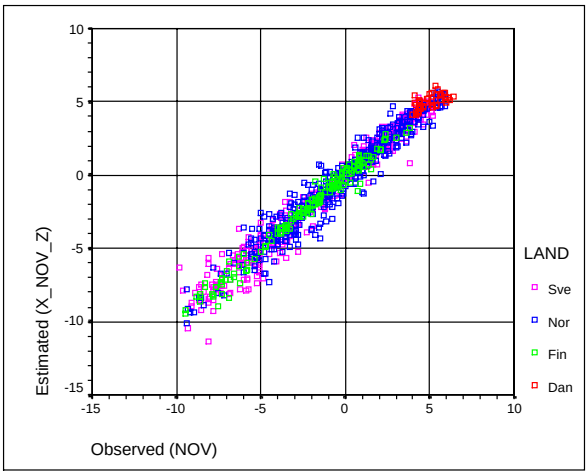

Figure 13a Observed vs. estimated temperature, Nov.

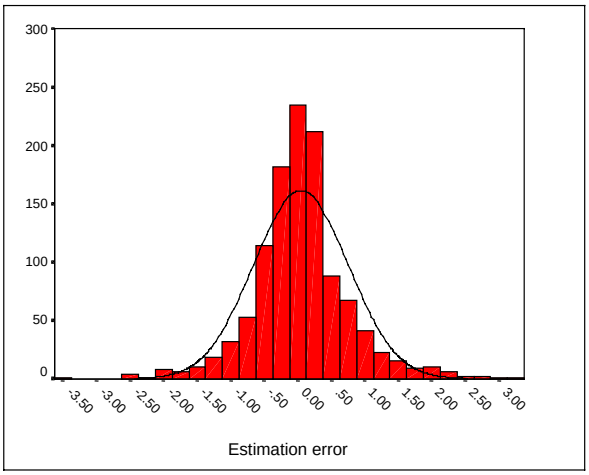

Figure 13b Frequency of estimation errors, Nov.

Defining and verifying trend components for Icelandic temperatures

Since Iceland is located far away from the other Nordic countries, and is surrounded by ocean, its temperature conditions have to be analysed separately.

The same parameters as for Fennoscandia were used to find the trend component, but since distances are shorter, mean (DEM_MEAN10) and minimum (DEM_MIN10) altitude within a 10km radius was also applied.

As for Fennoscandia, the influence of the trend parameters varies throughout the year. The most important variables in the trend expressions are altitude and latitude, which are included for all months. Mean altitude and longitude contributes in the summer season. Table 4 shows the regression coefficients and statistics for Icelandic temperatures.

Table 4: Regression coefficients and statistics for Icelandic temperature normals.

	ALT	DEM_MEAN	DEM_MEAN10	LAT	LONG	Const	R	R^2	S.E.
Jan	-0.0097			-0.708		45.001	0.87	0.76	0.85
Feb	-0.0096			-0.864		55.757	0.90	0.81	0.75
Mar	-0.0089			-1.073		69.337	0.94	0.88	0.60
Apr	-0.0097		0.0015	-1.153		76.774	0.96	0.93	0.42
May	-0.0093		0.0030	-1.142	-0.0814	77.546	0.92	0.85	0.57
Jun	-0.0079	0.0040		-0.767	-0.0756	56.047	0.81	0.65	0.70
Jul	-0.0071	0.0038		-0.760	-0.0898	56.962	0.82	0.66	0.63
Aug	-0.0070	0.0025		-0.674	-0.0643	51.762	0.89	0.78	0.46
Sep	-0.0075		0.0008	-0.748		55.211	0.95	0.91	0.36
Oct	-0.0080			-0.659		46.654	0.92	0.85	0.54
Nov	-0.0094			-0.556		36.843	0.88	0.78	0.77
Dec	-0.0094			-0.644		41.063	0.87	0.75	0.82

Compared to Fennoscandia, the coefficients for altitude are different. The lapse rate is close to the dry-adiabatic rate -1°C/100 m a.s.l. in the winter season, despite the fact that inversions occur frequently. These inversions are however shallow, and are easily mixed up under windy conditions. Due to the relatively high ocean temperatures, the temperature gradient above the inversion layer is close to the adiabatic lapse rate.

During the summer season, the air is generally stable, and the temperature gradient is consequently closer to the standard lapse rate towards summer. During the summer season, also the large scale terrain (DEM_MEAN) contributes.

The standard error of the trend expressions for Icelandic mean temperatures are lower than 1°C for all months, reflecting quite homogenous temperature conditions. The resulting de-trended temperatures show generally small systematic variations. In January (Figure 13, top map), the temperatures at the western and eastern coasts are systematically too high, as well as temperatures at stations located on islands. Except for the kriging estimates at the islands Vestmannaeyar and Grimsey, the estimation errors are within ±2°C (Figure 13, lower map). The distribution of the final estimates is shown in figure 14, and shows very good fit.

For April, the score is even better. Most of the estimates are within ±1°C (Figure 15).

The summer months June and July have the lowest score explaining the trend. The de-trended temperature shows almost no systematical spatial variation (Fig. 16). The experimental semivariogram (Figure 17) reveals clearly the random spatial conditions. Instead of fitting a theoretical semivariogram, the mean de-trended temperature could have been used. In this case a semivariogram with short range is applied, giving the nearest station more weight than stations further away. The distribution of estimation errors (figure 18) shows the existence of a few large deviations, especially at the eastern coast.

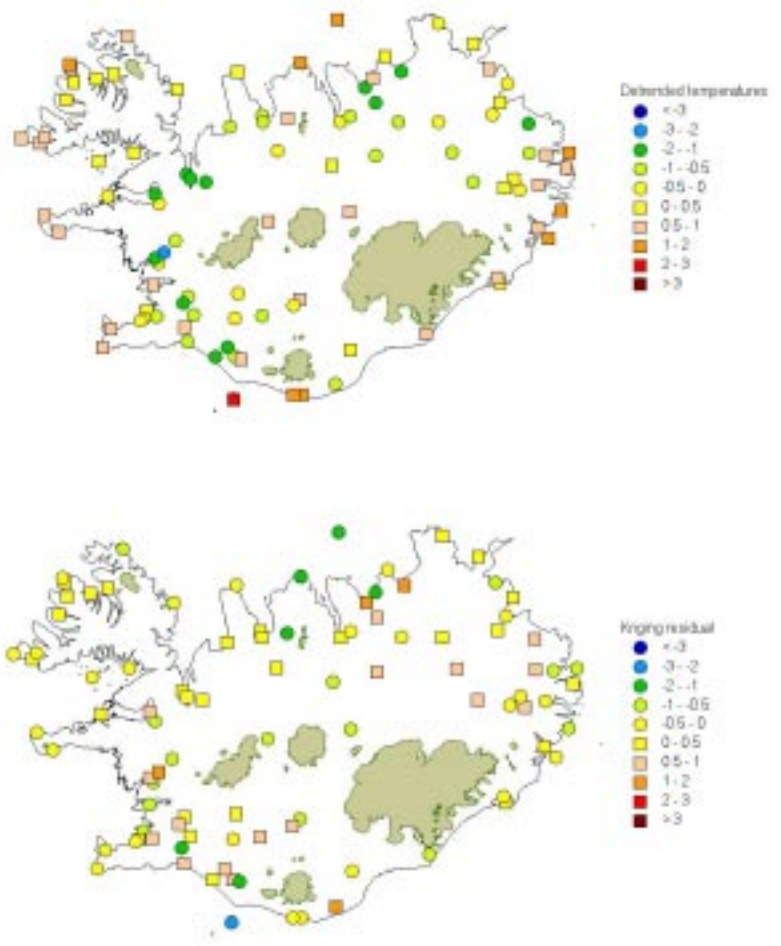

Figure 13. Detrended temperatures and kriging residuals for Iceland in January.

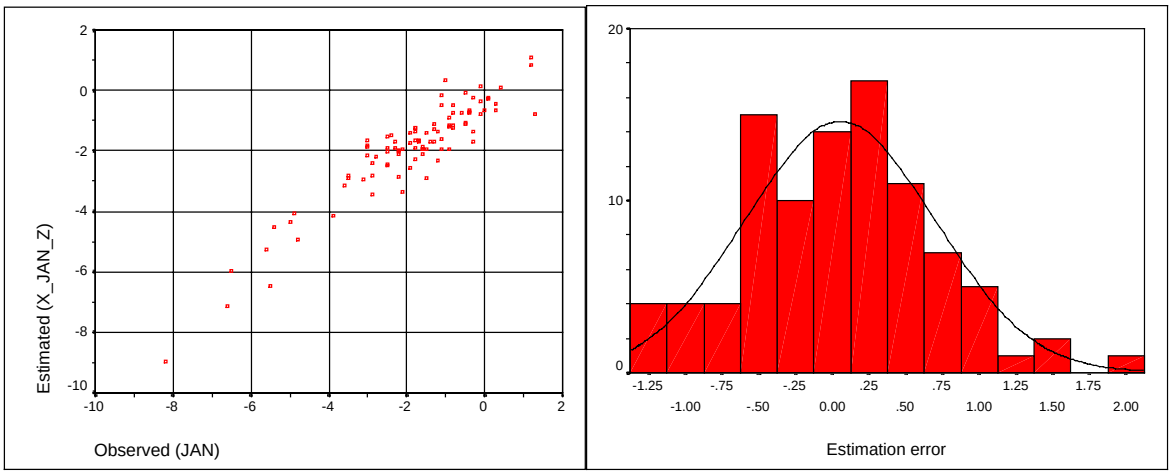

Figure 14. Distribution of estimation errors for Icelandic temperatures in January.

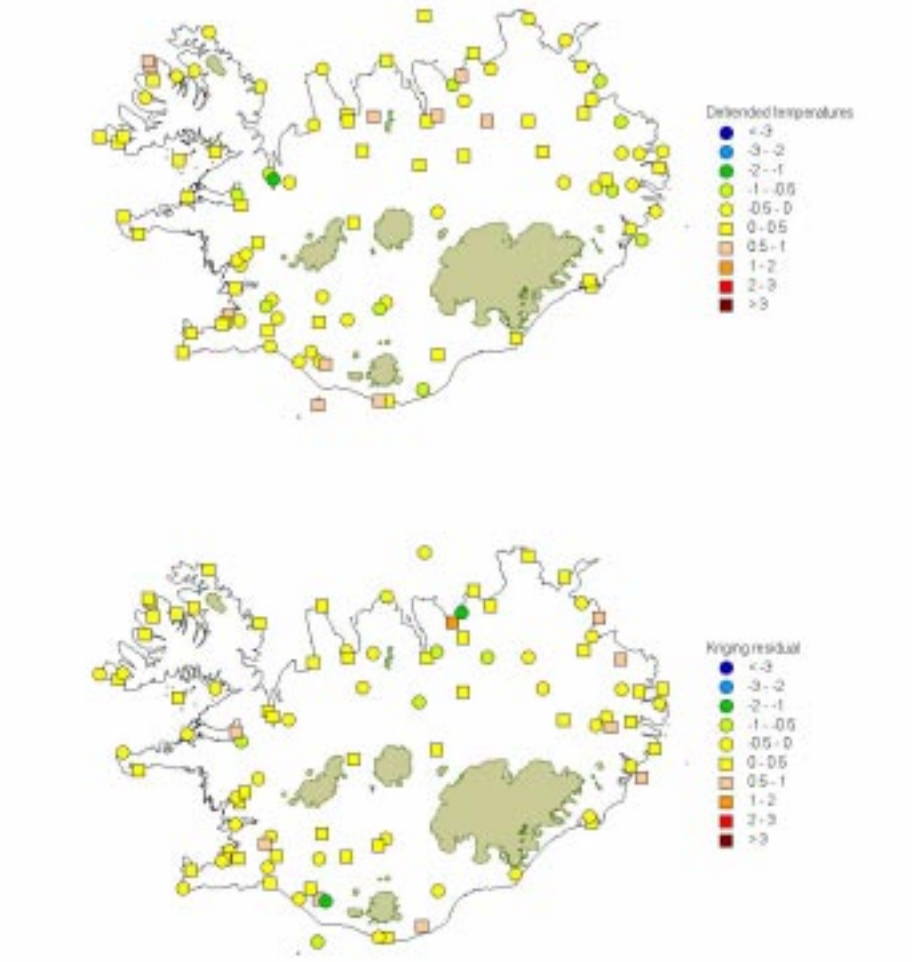

Figure 16. Detrended temperatures (upper) and kriging residuals (lower) for Iceland in July.

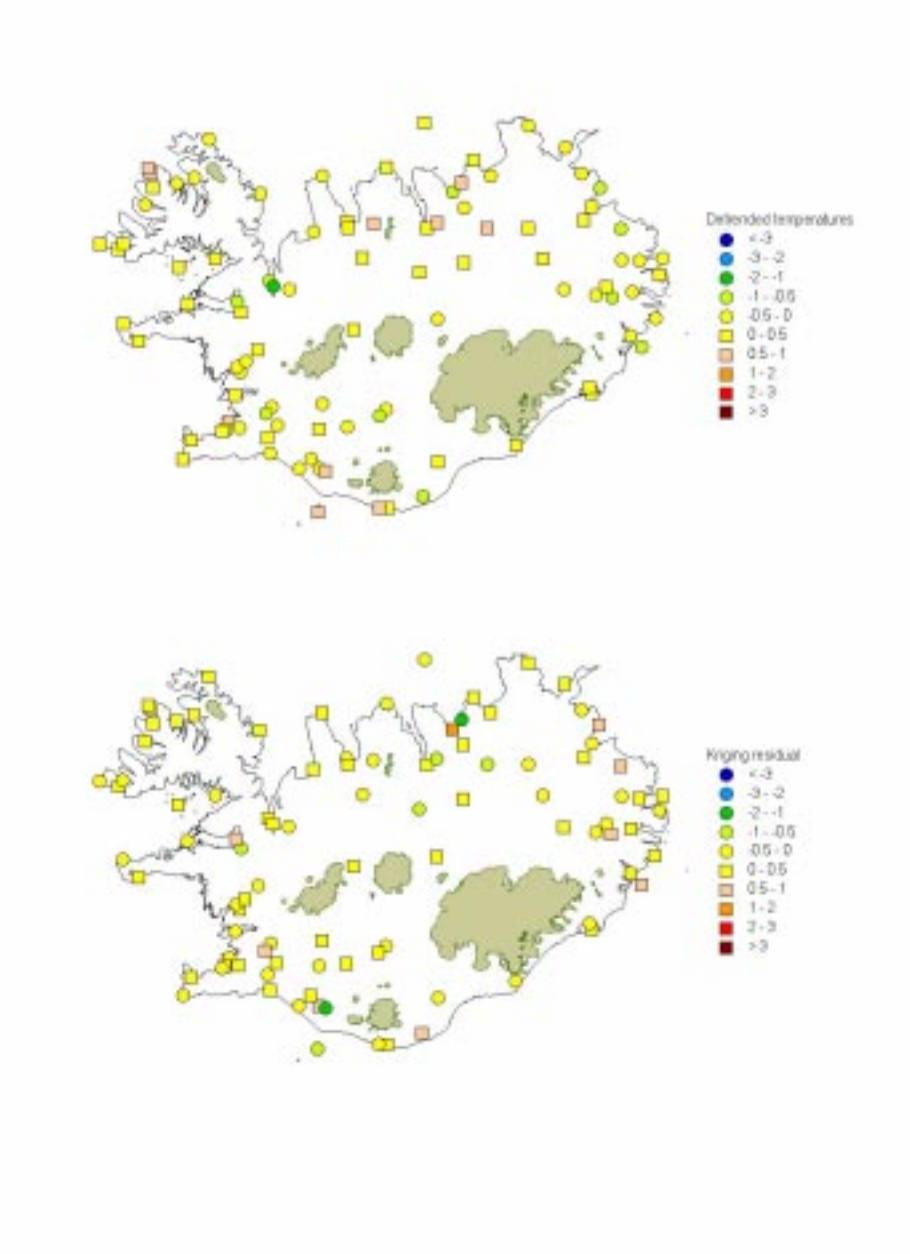

Figure 16. Detrended temperatures (upper) and kriging residuals (lower) for Iceland in July.

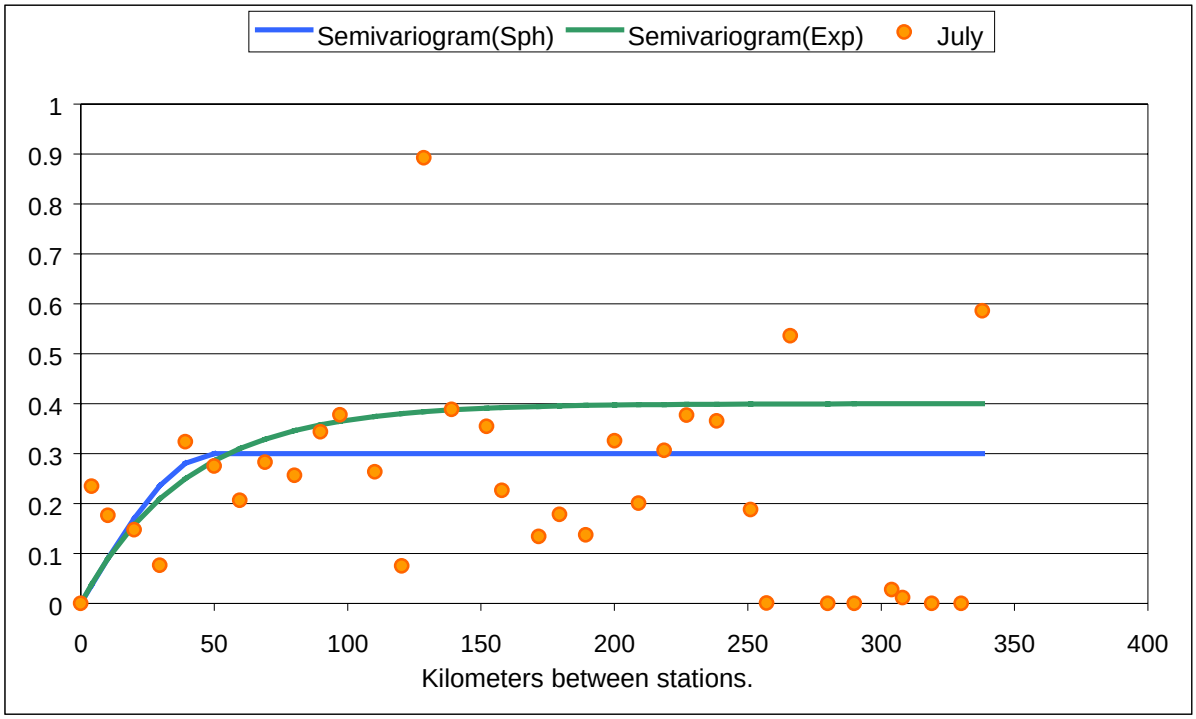

Figure 17. Semivariogram of detrended temperatures in Iceland in July.

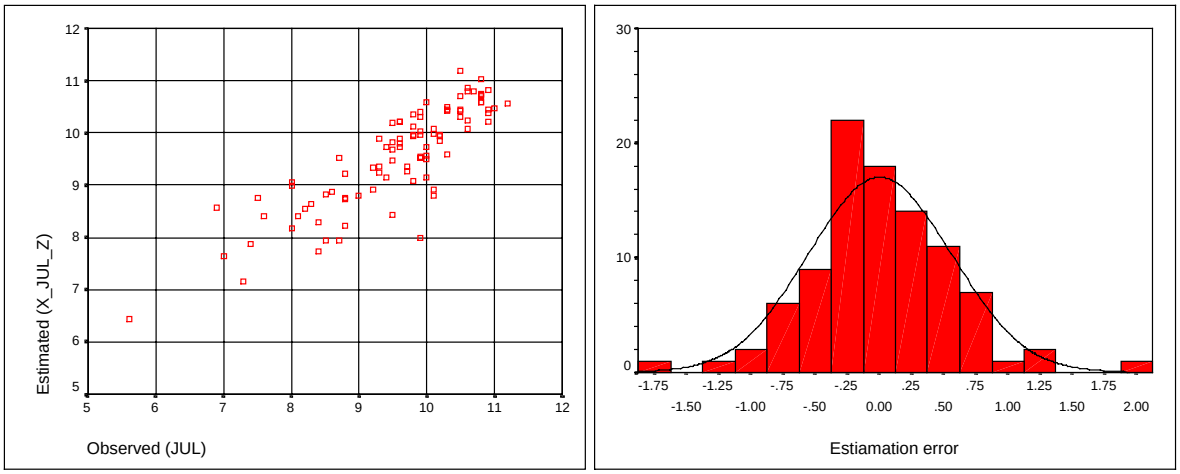

Figure 18. Distribution of estimation errors for Icelandic temperatures in July.

Temperature climate in the Nordic region

General description

The main factor influencing the temperature climate in the Nordic region is the geographical position in the Eurasian continent's coastal zone, which shows characteristics of both a maritime and a continental climate, depending on the direction of air flow. Since the Nordic countries are located in the zone of prevailing westerly, mild airflows from the Atlantic Sea which are warmed by the Gulf Stream, are dominant. The mean temperature is therefore several degrees (more than 10°C in winter) higher than that of other areas in the corresponding latitudes. The open waters of the Baltic Sea and large lakes also contribute to raising the winter temperature.

Fennoscandia is characterized by several mountain ranges, especially in south-western Norway and along the border between Norway and Sweden. When saturated air is lifted over a mountain range, the temperature at the (humid) windward side of the mountains will decrease with approximately 5ºC/km. If the moisture precipitates at windward side, the dry air will be warmed by 10ºC/km on the leeward side of the mountains. This is called the "föhn"-effect. In situations where westerly winds prevail, the weather is usually warm in most of the region emphasised by this phenomenon. Despite the moderating effect of the ocean, the Asian continental climate also extends to the Nordic region at times, manifesting itself as severe cold in winter and extreme heat in summer.

The climate of the Nordic countries is strongly influenced by the polar front, where tropical and polar air masses meet. The temperature can thus change quite rapidly, particularly in winter. The systems known to affect the weather are the low-pressure system usually found near Iceland and the high-pressure systems in Siberia and the Azores. The position and strength of these systems vary, and any one of them can dominate the weather for a considerable time.

According to Köppen's climate classification (Eliassen and Pedersen, 1977), the mainland of the Nordic region belongs mostly to the temperate coniferous-mixed forest zone with cold, wet winters.

Annual, seasonal and monthly temperatures

The mean annual temperature map is presented in Chapter 4. Annual temperature decreases basically according to the latitude, but the ocean and mountain areas have a great influence on the temperature distribution. The maximum annual station values are 8.4°C at coastal stations in southern Denmark, while the lowest station value is **–17.3**°C at Vittangi, a mountain station in Northern Sweden.

The annual range of mean temperature i.e. the difference between the mean temperatures of the warmest and coldest month of the year, is generally regarded as a measure of continentality of the region and several continentality indices are based on it. The spatial distribution of the annual range during the normal period 1961-90 (cf. next chapter) is characterised by the lowest values (about 10°C) at lighthouses at the Norwegian coastline, while the most continental areas (up to 31°C) are in Lapland.

The figures in the next chapter show mean temperatures for each season and month.

Thermal seasons

In addition to the normal calendar seasons, which the maps in this report refer to, it is natural to distinguish between seasons using thermal criteria, with seasons separated by the daily mean temperatures of 0°C and 10°C. The following brief considerations include only Finnish, Norwegian and Swedish mainland regions, basing at the maps published in the National Climate Atlases of each country.

Spring

In spring, the mean daily temperature rises from 0°C to 10°C. It begins, on average, already in the first half of February in south-western regions, but as late as May in northern inland areas. Once the mean daily temperature exceeds 5°C, the thermal growing season is considered to have begun. This takes place 1-2 months after the beginning of the thermal spring.

Summer

In summer, the mean daily temperature is consistently above 10°C. Summer usually begins in the first half of May, but not before the end of June in northern inland areas. The highest summer temperatures in the southern interior regions may be around 35°C. Near the sea and on the islands, temperatures over 30°C are rare. The highest temperature recorded in 1961-1990 is 36.8°C (Holma, Sweden, 9/8 1975)**.**

Autumn

In autumn, the mean daily temperature remains below 10°C. Autumn begins in early August in northern inland areas, but delays until mid-October in south-western regions. The growing season ends in autumn when the mean daily temperature drops below 5°C. This occurs around early September in northern inland regions and as late as November in south-western coast regions.

Winter

Winter (mean temperature below 0°C) usually begins in mid-October in Lapland, but not until January in the south-western areas. The sea (and also lakes) retard the progress of winter. The coldest day of winter comes in the turn of January-February except in the coastal regions, where the slower cooling of the sea delays the coldest period until later February. The lowest temperatures in winter are less than -50°C. The lowest temperature recorded in the region in 1961-1990 is – 52.6°C (Vuoggatjålme, Sweden, 2.2.1966).

Temperature maps

Mean January temperature 1961-90

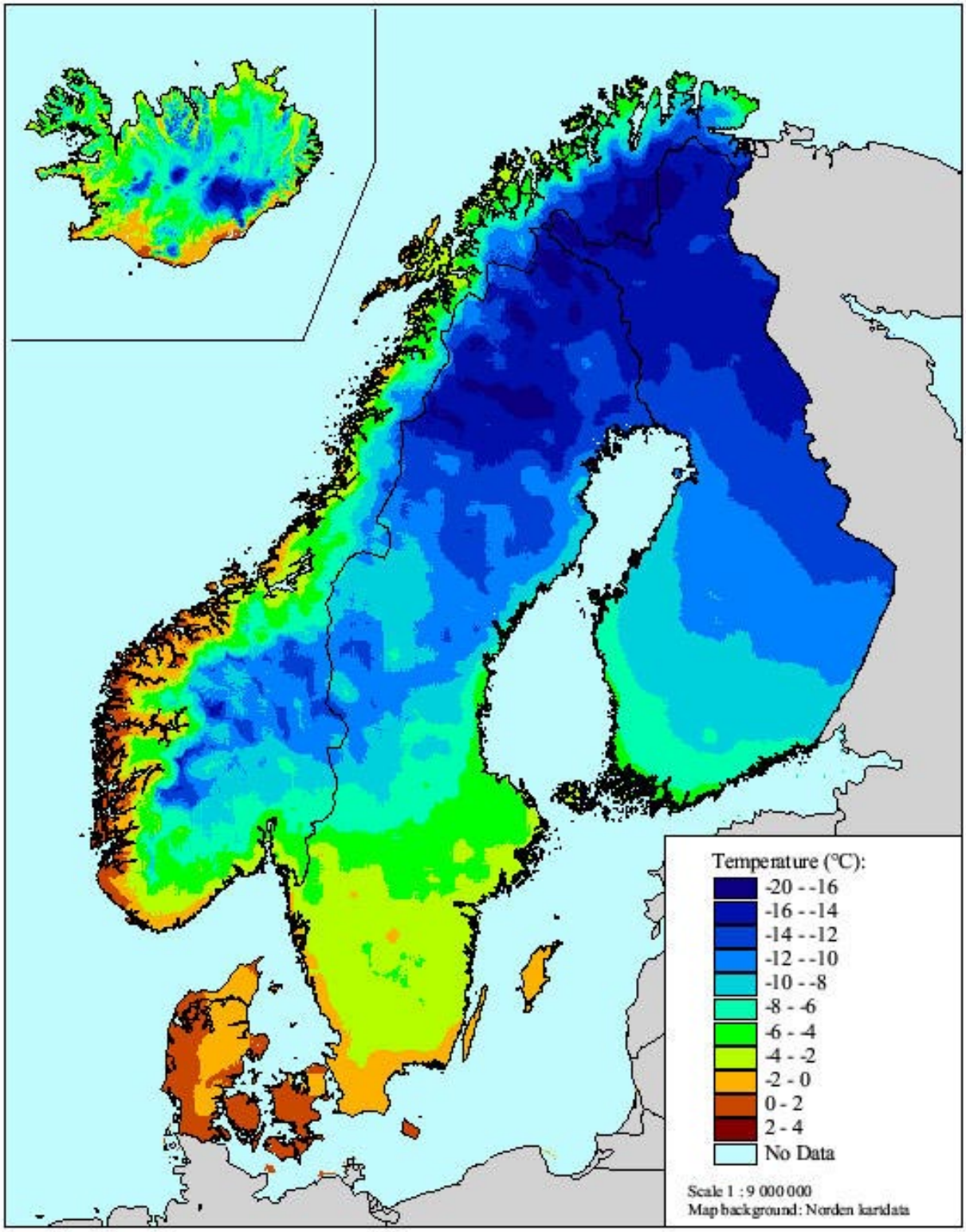

Mean February temperature 1961-90

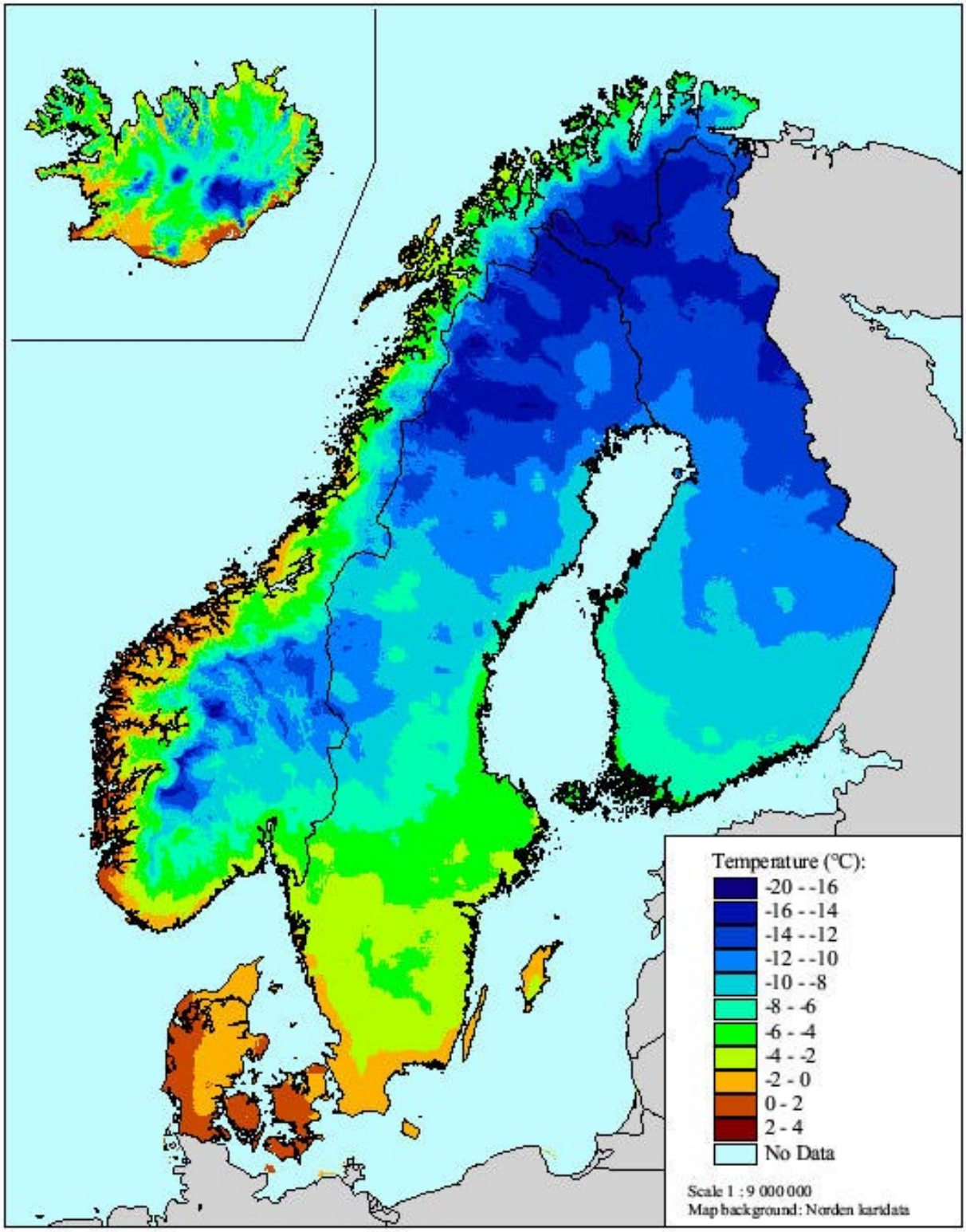

Mean March temperature 1961-90

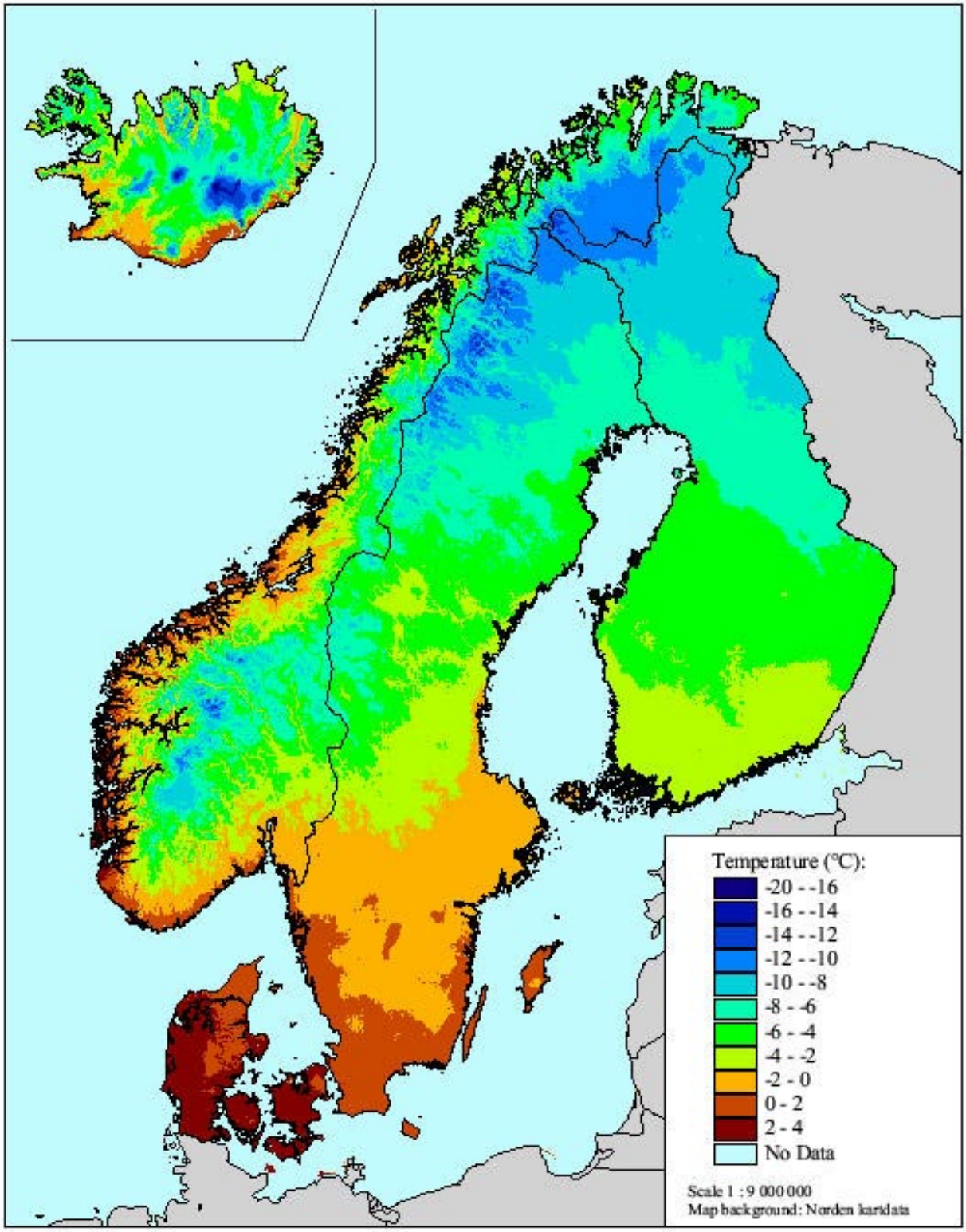

Mean April temperature 1961-90

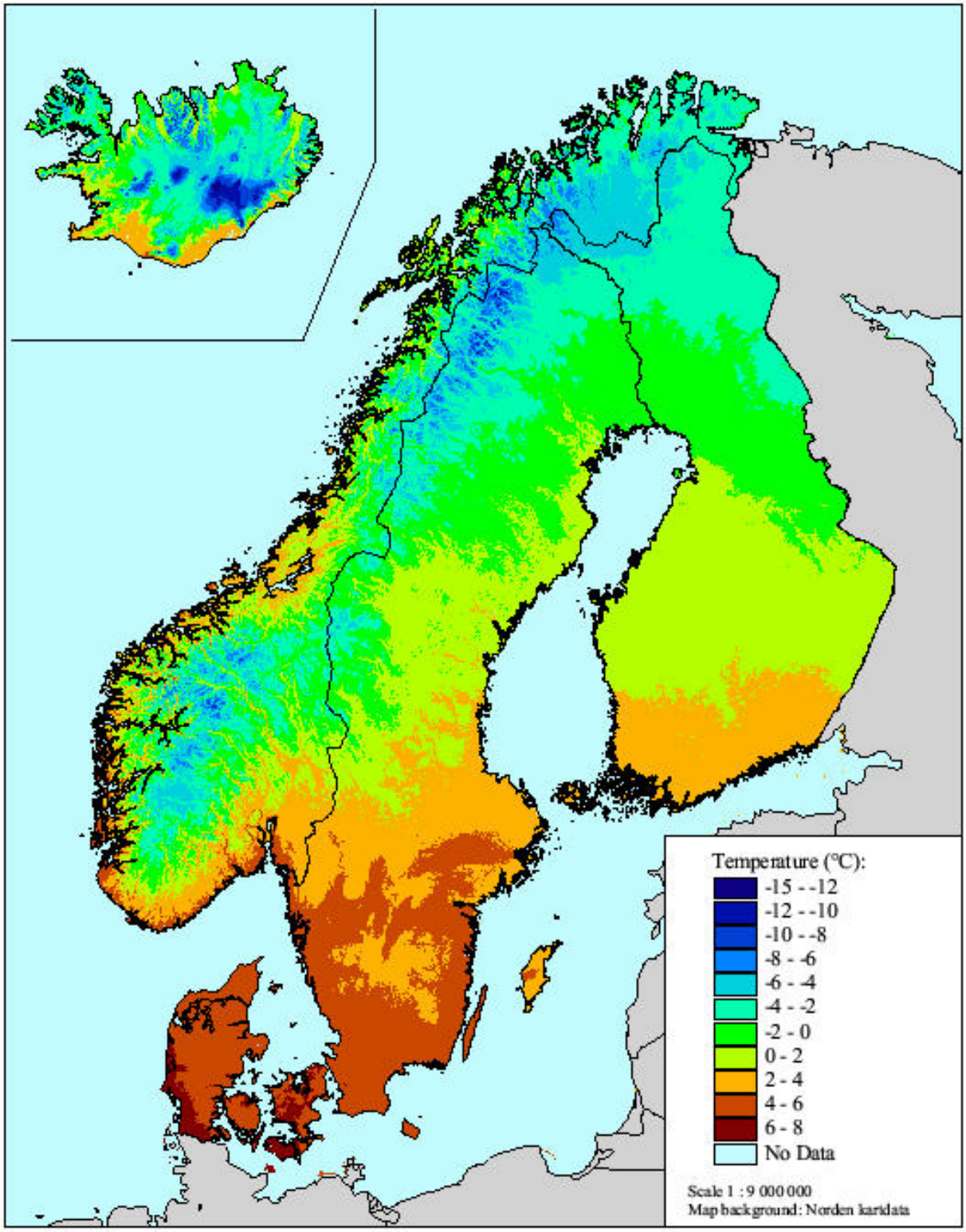

Mean May temperature 1961-90

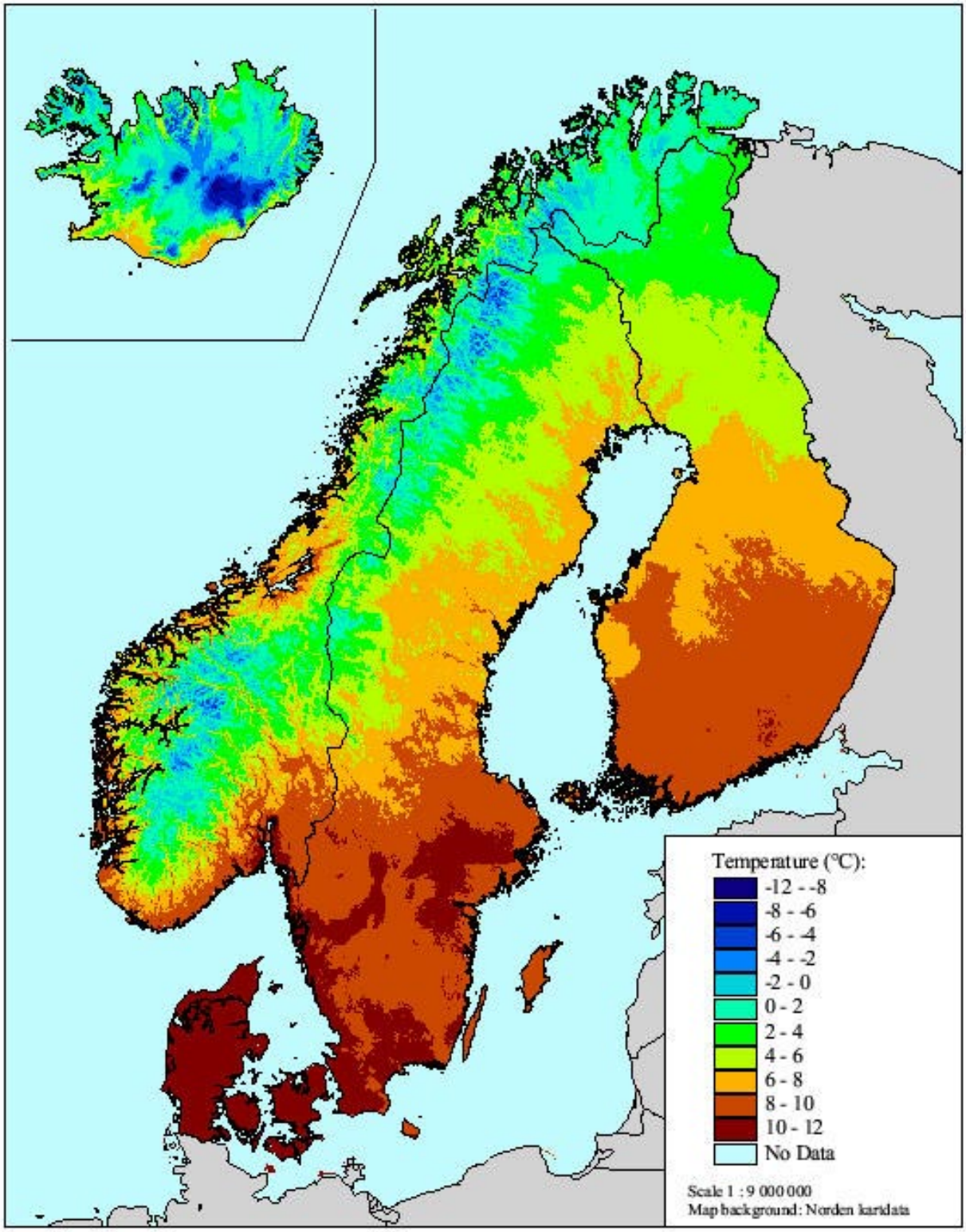

Mean June temperature 1961-90

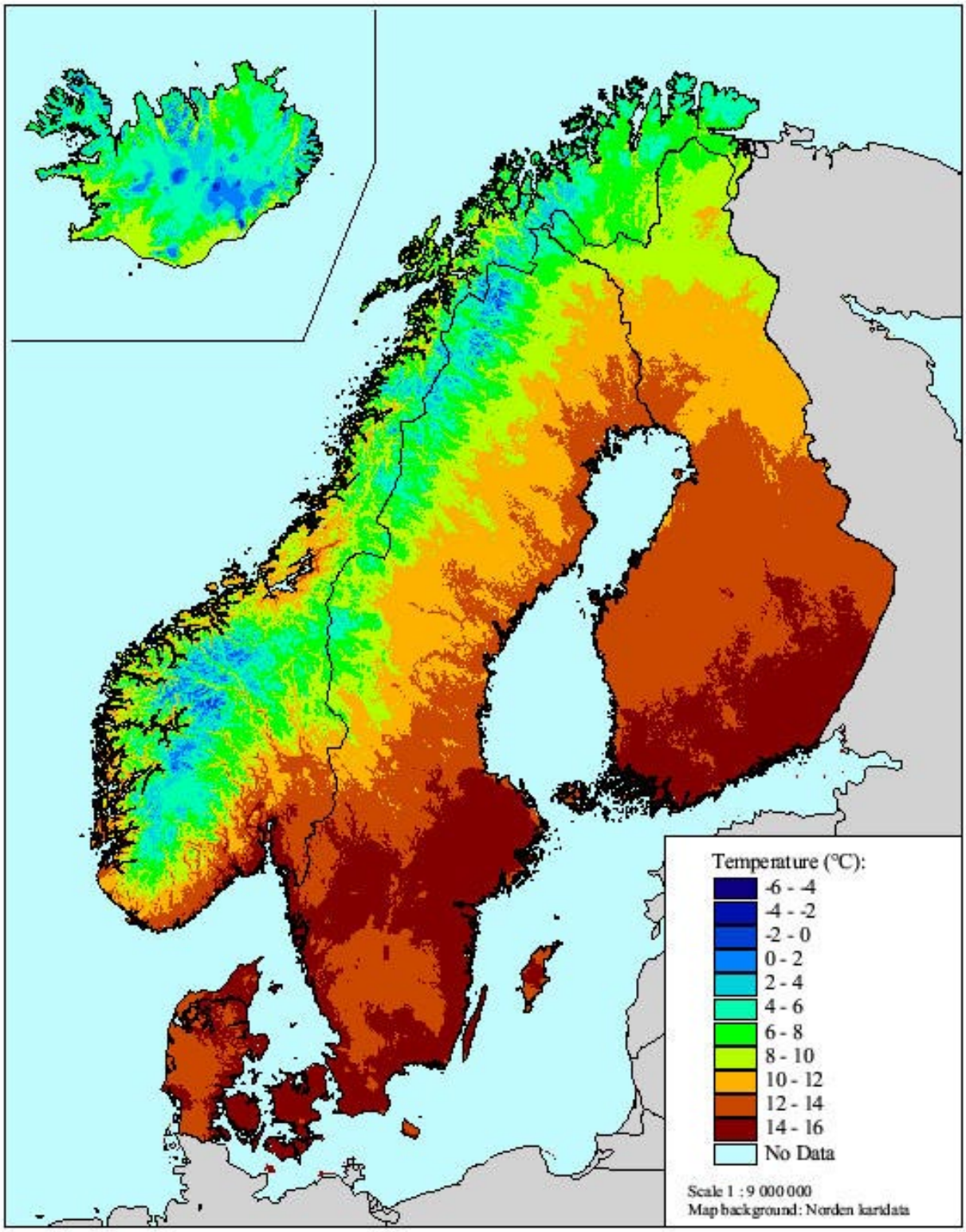

Mean July temperature 1961-90

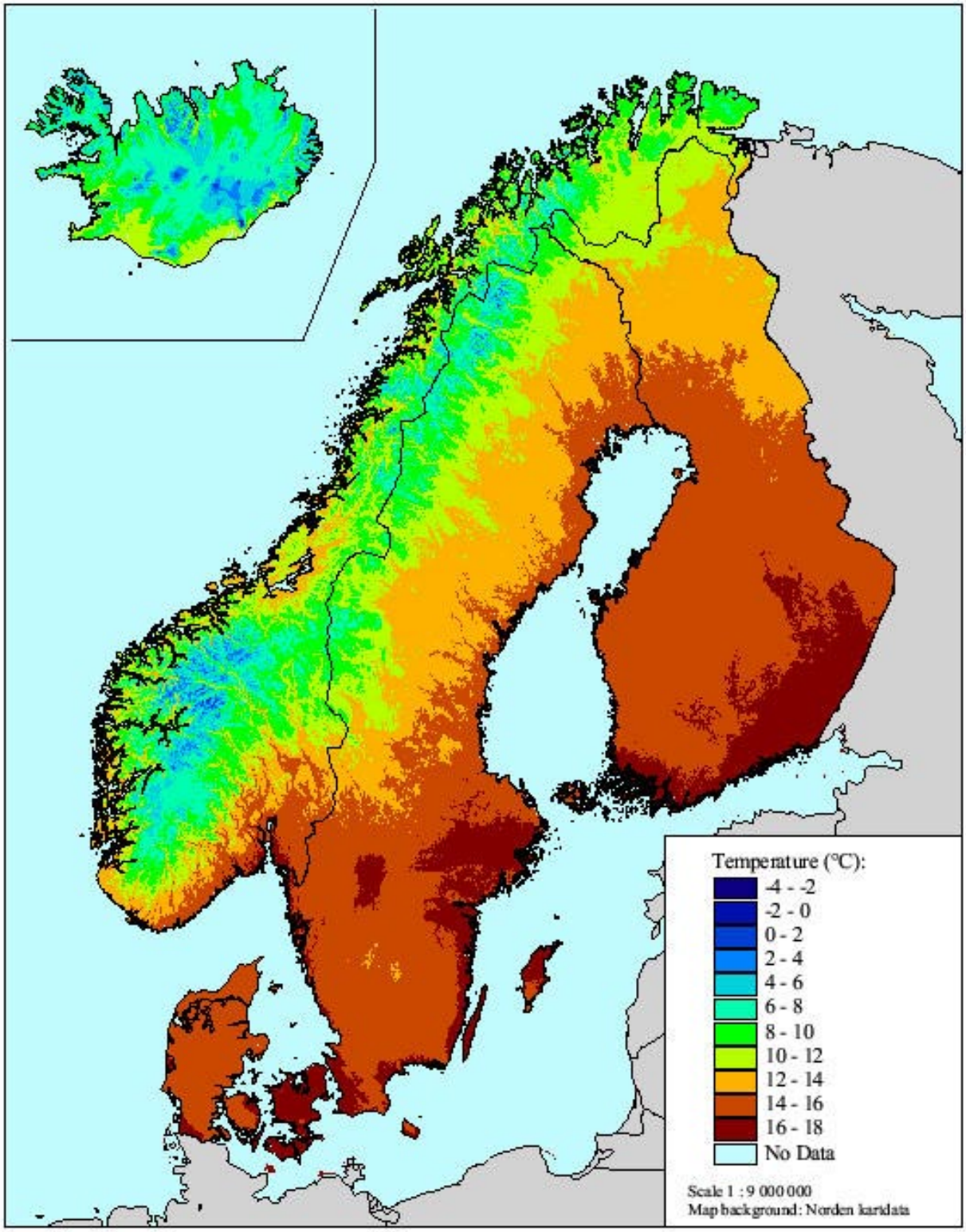

Mean August temperature 1961-90

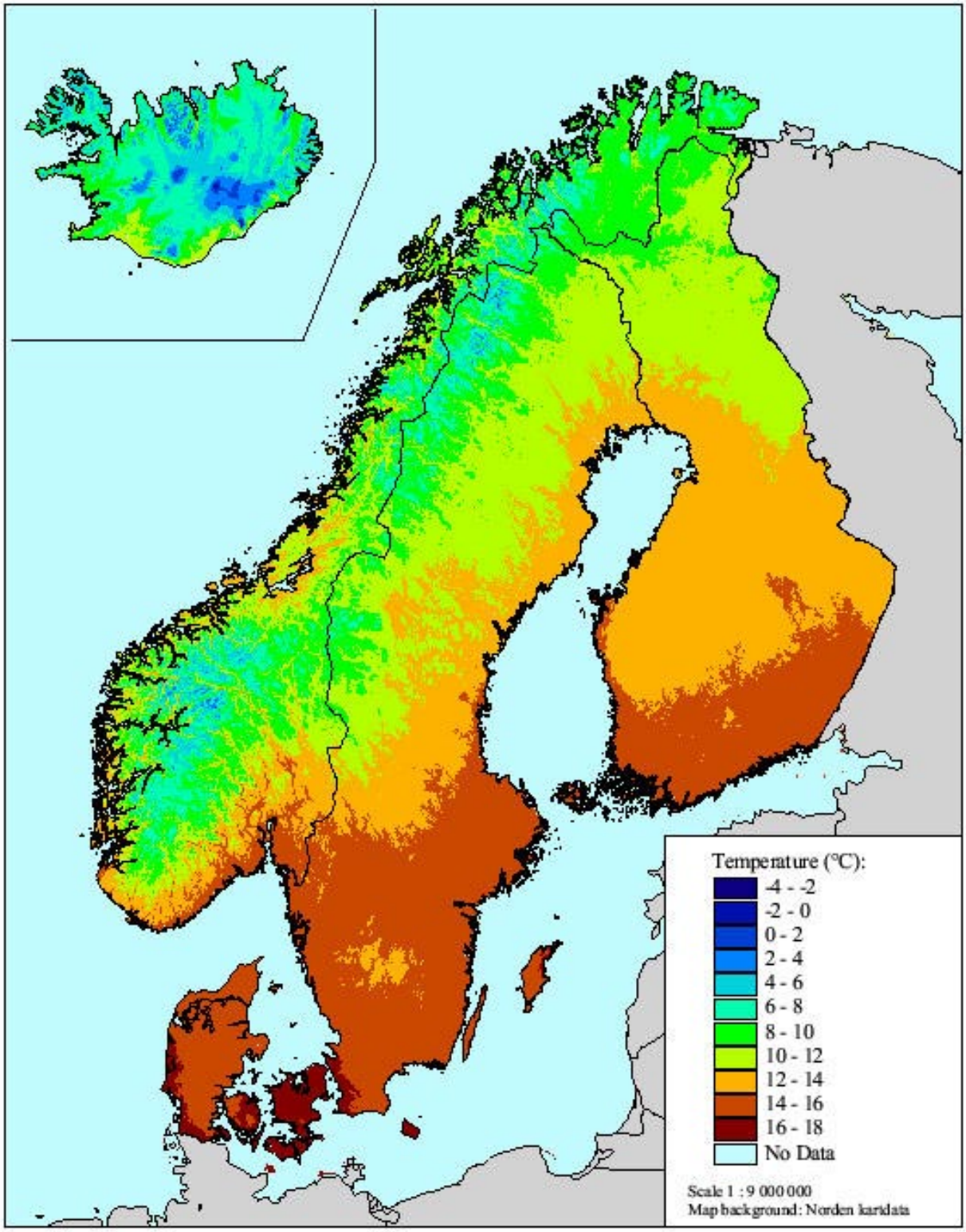

Mean September temperature 1961-90

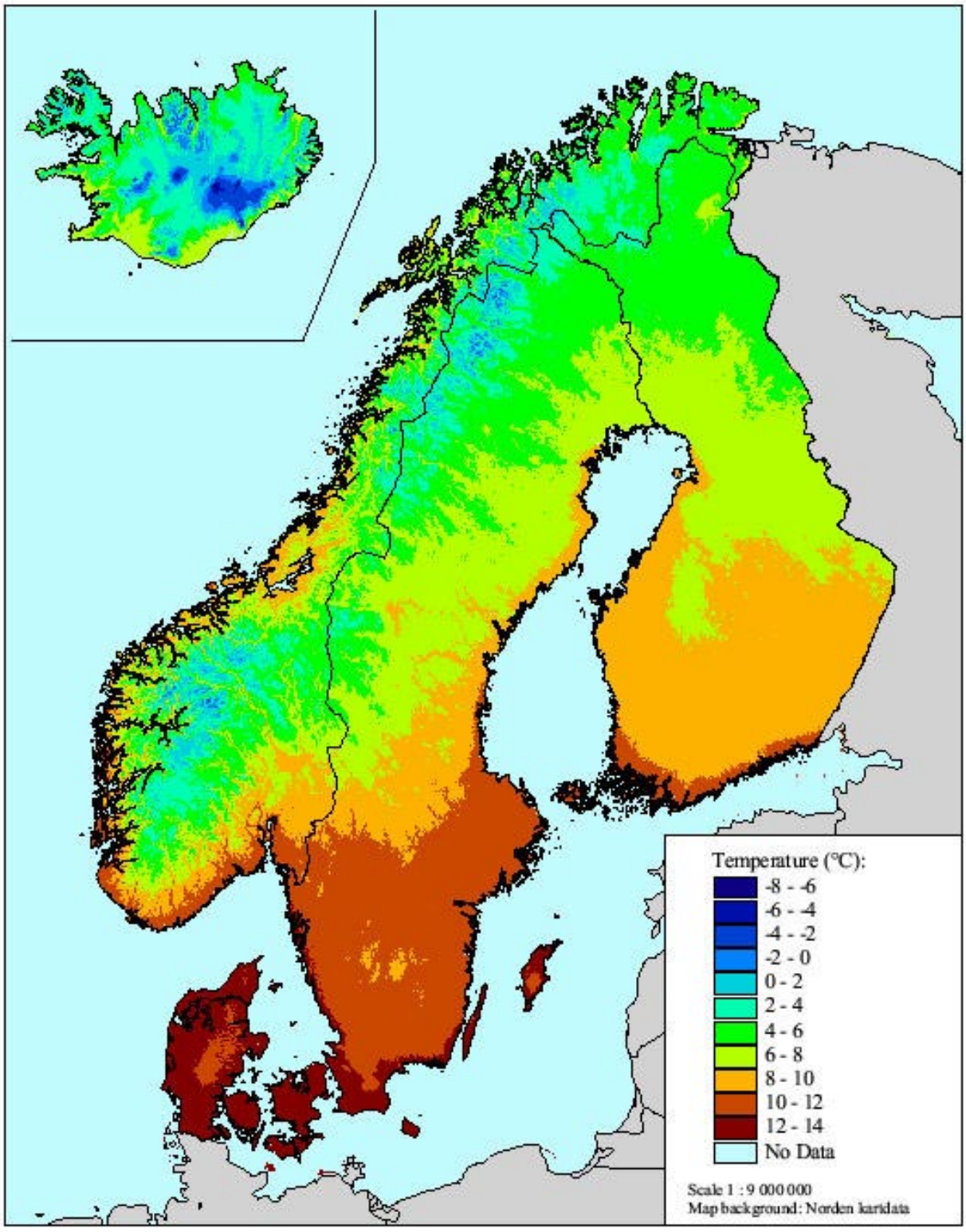

Mean October temperature 1961-90

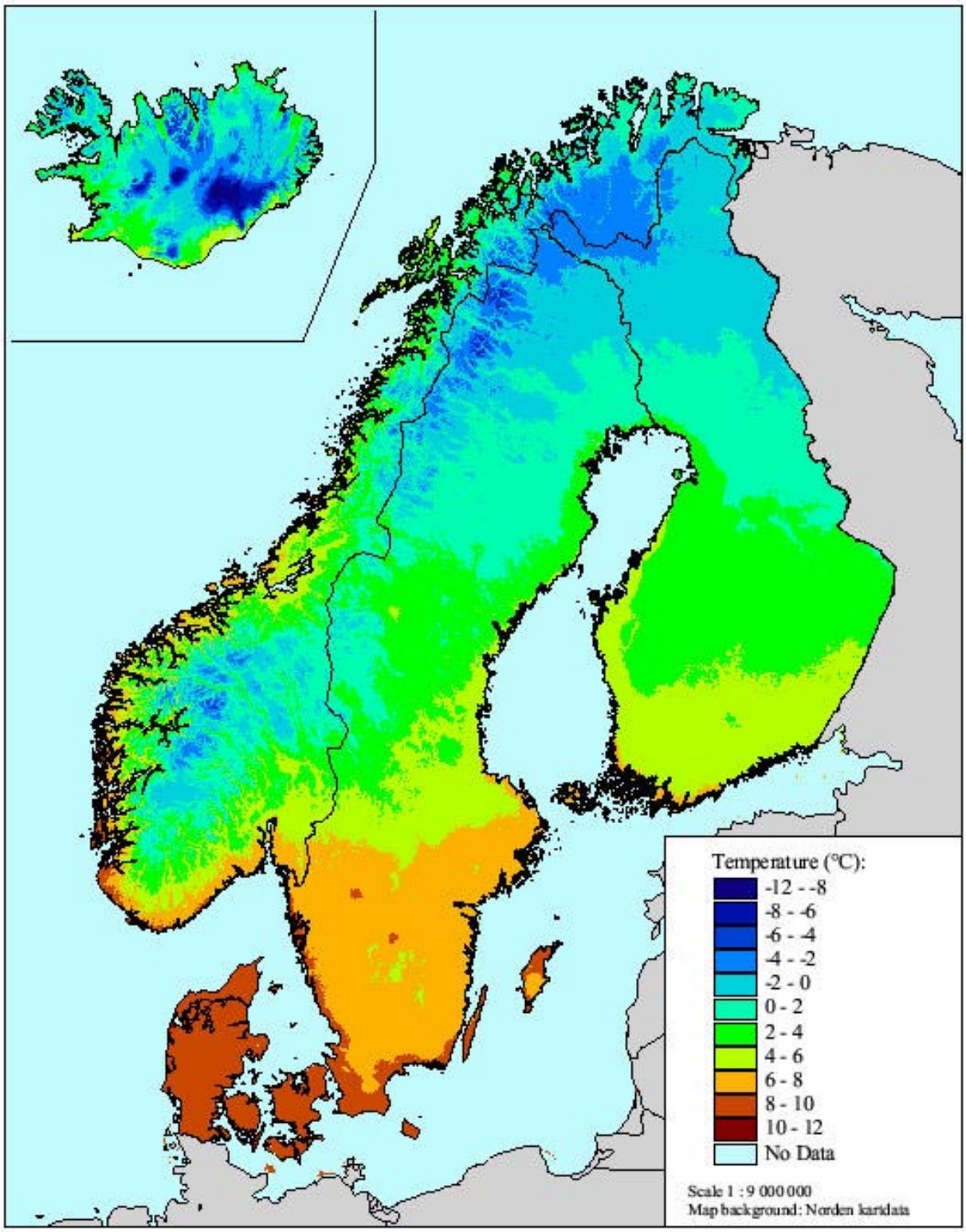

Mean November temperature 1961-90

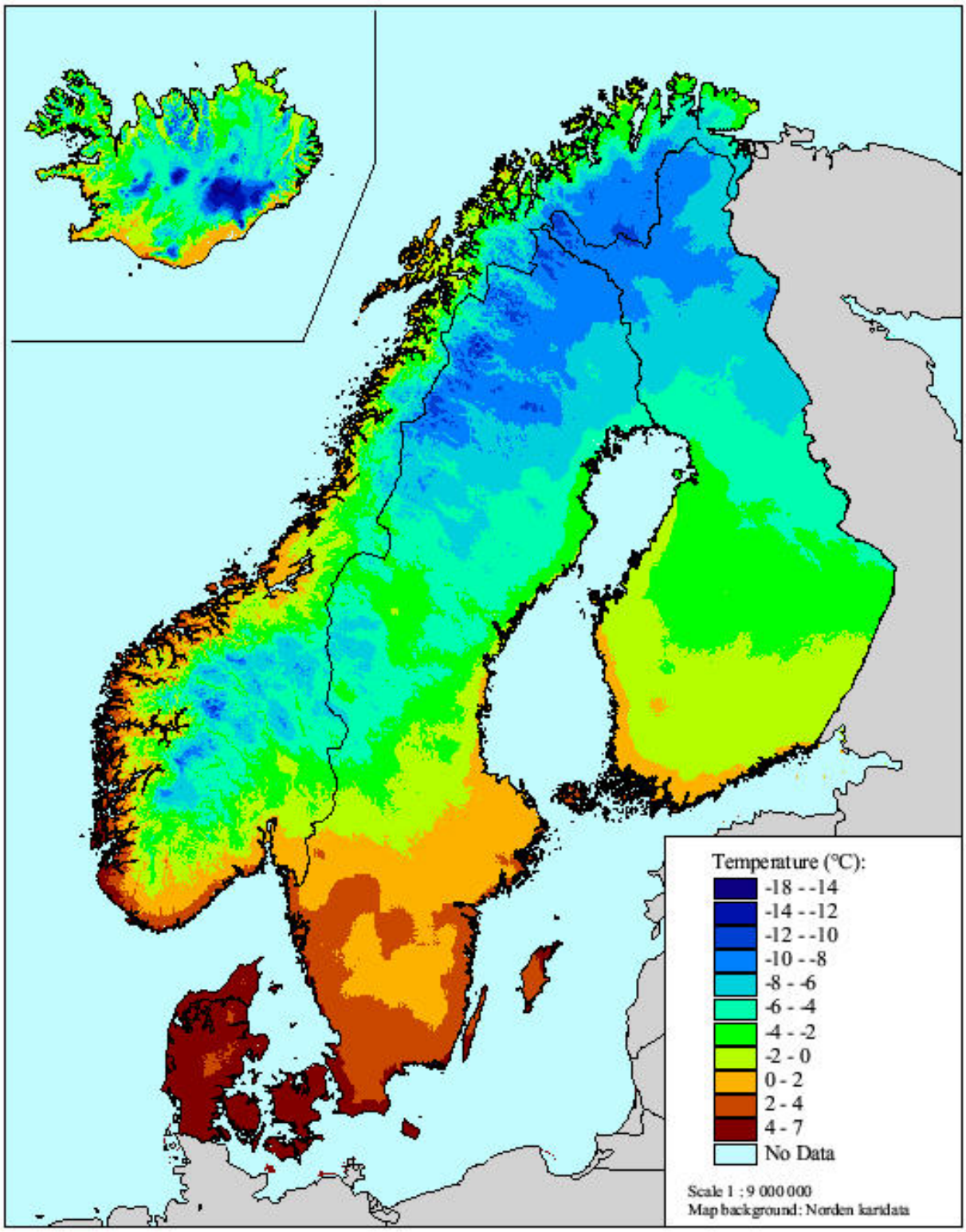

Mean December temperature 1961-90

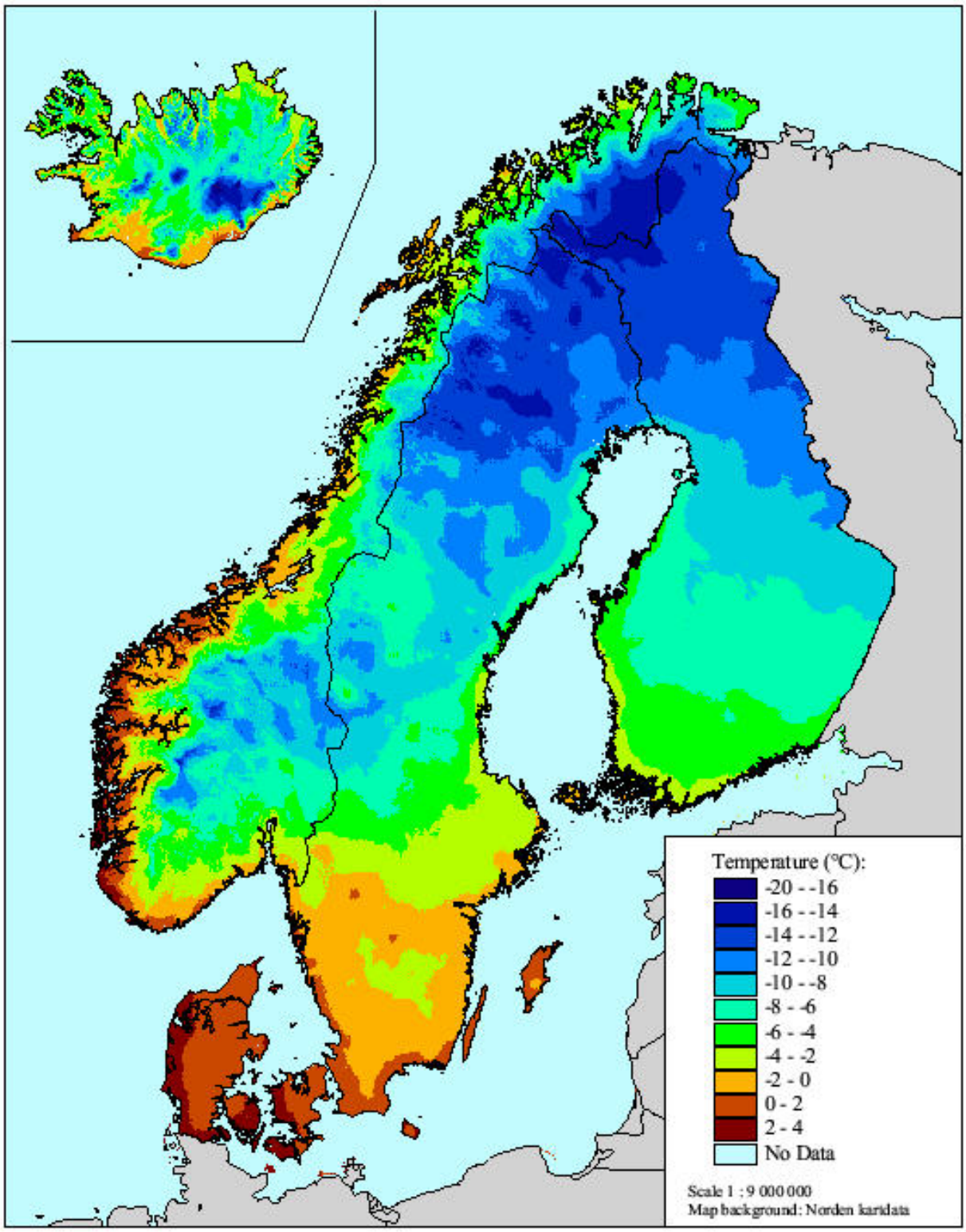

Mean annual temperature 1961-90

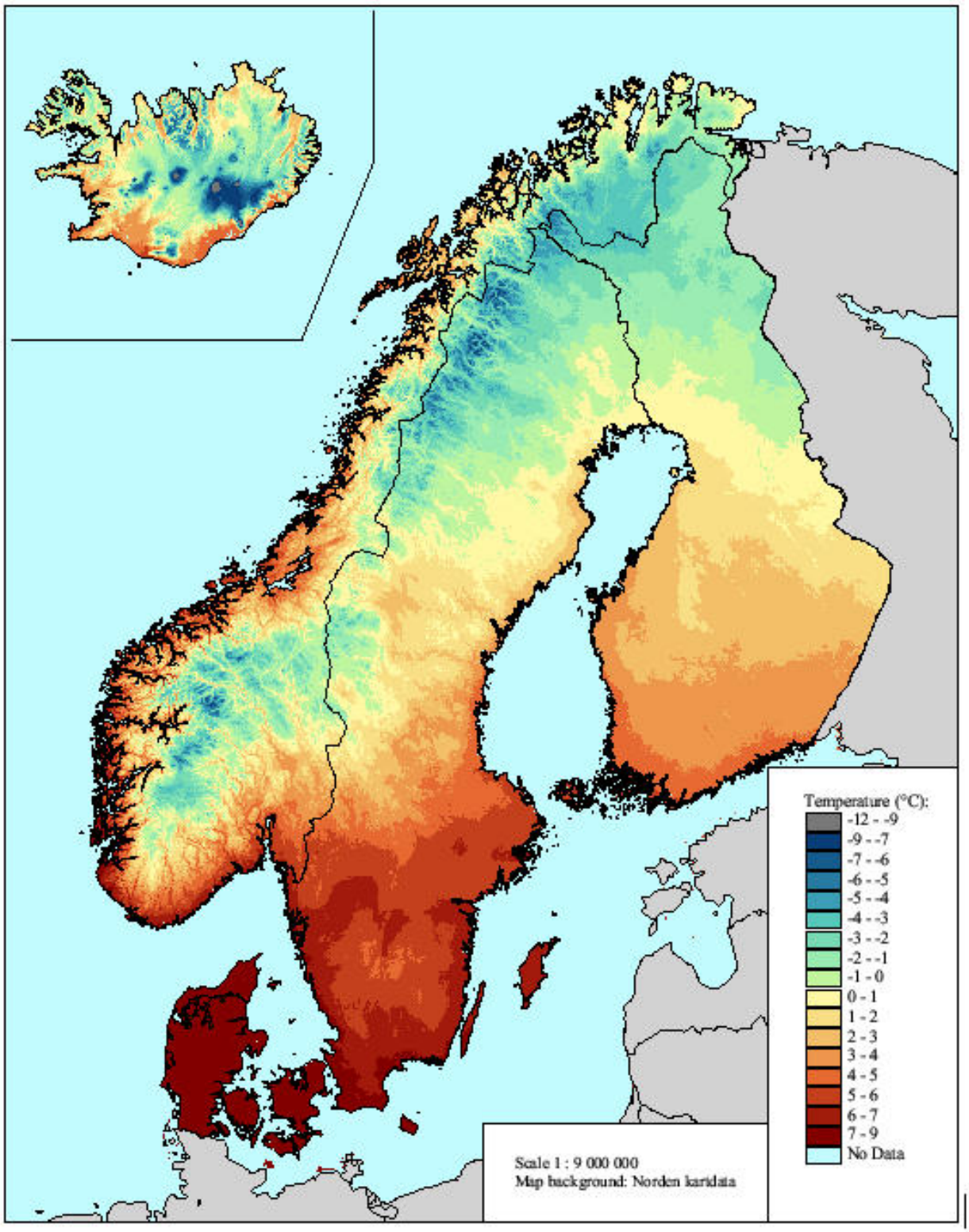

Mean winter temperature 1961-90

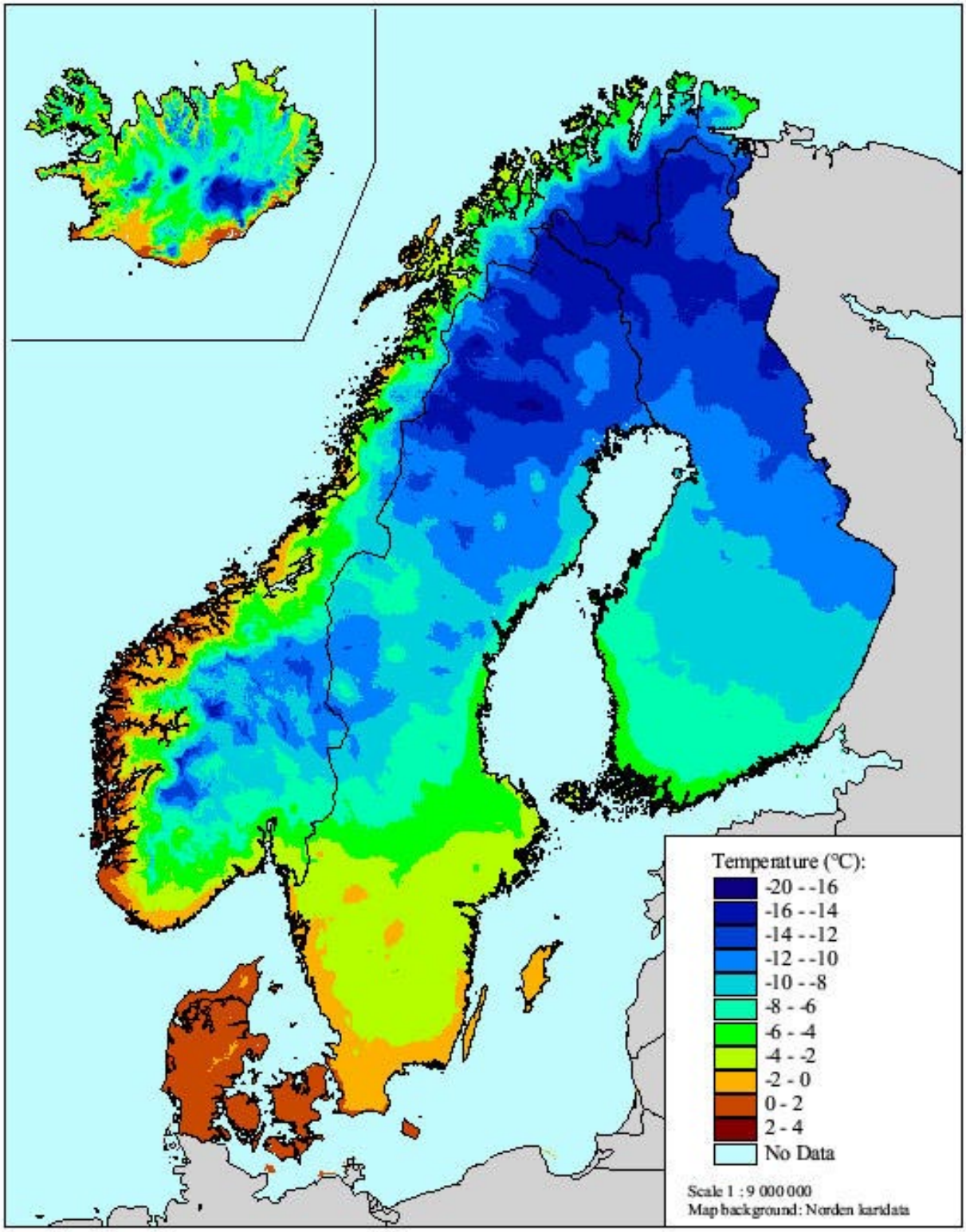

Mean spring temperature 1961-90

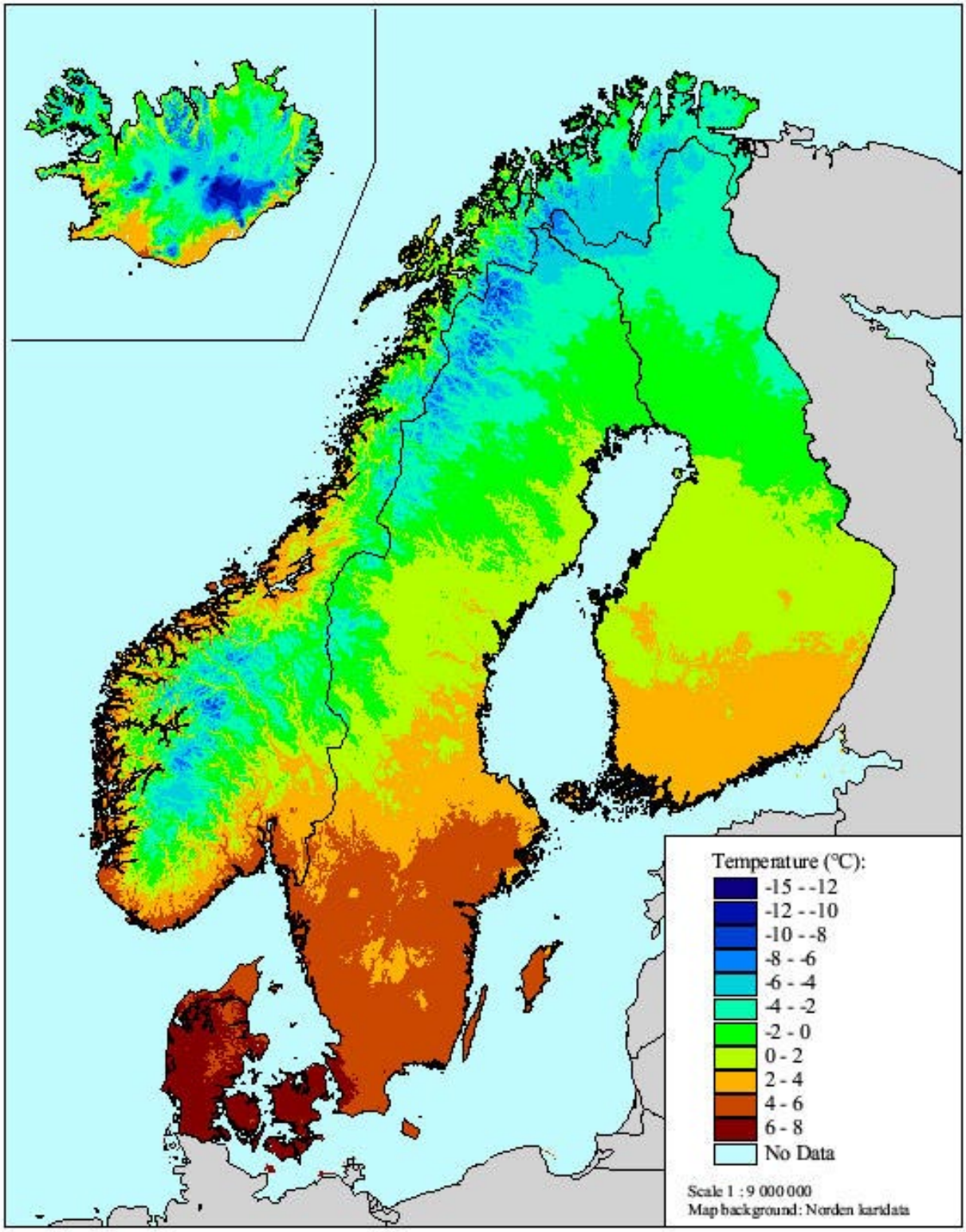

Mean summer temperature 1961-90

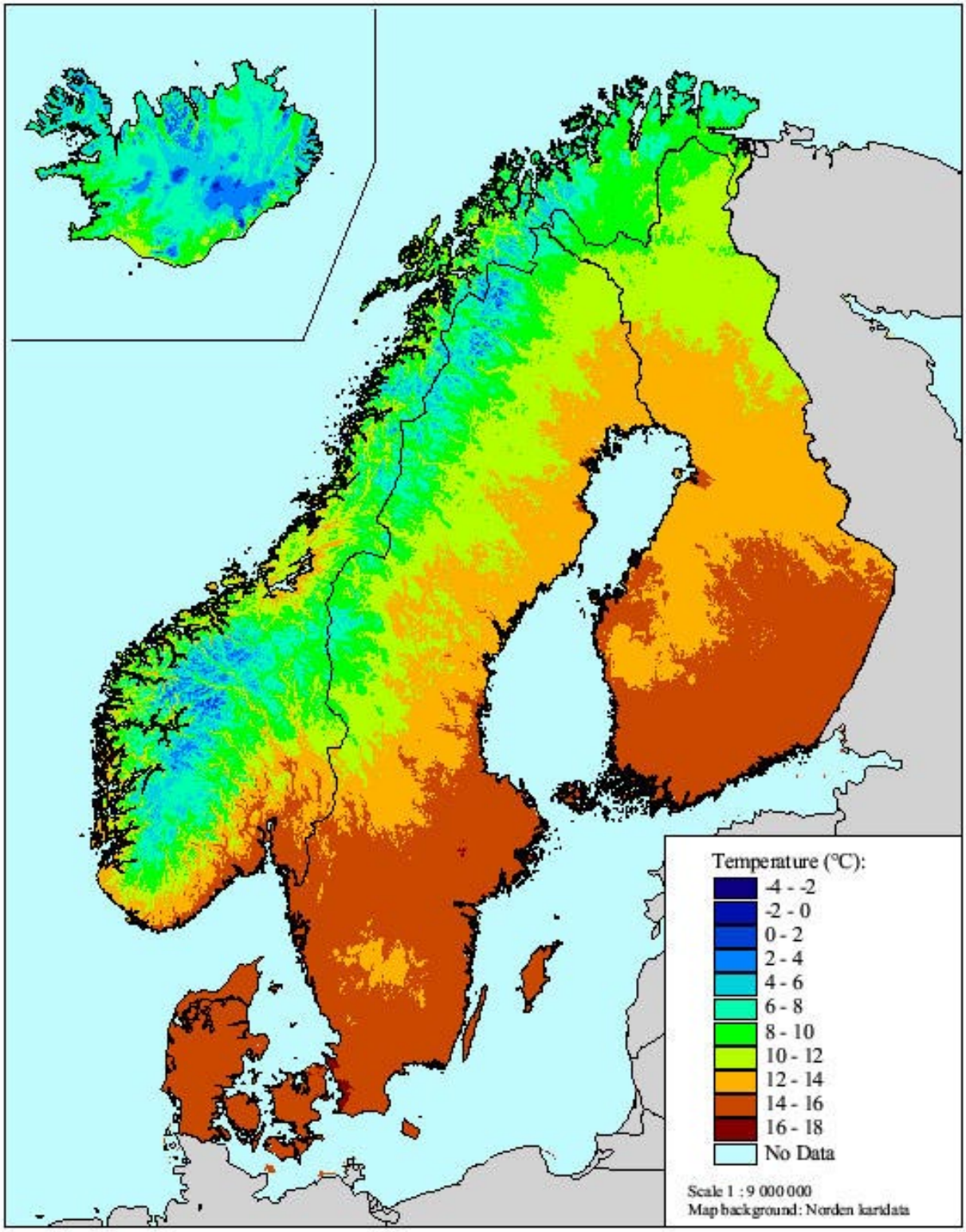

Mean autumn temperature 1961-90

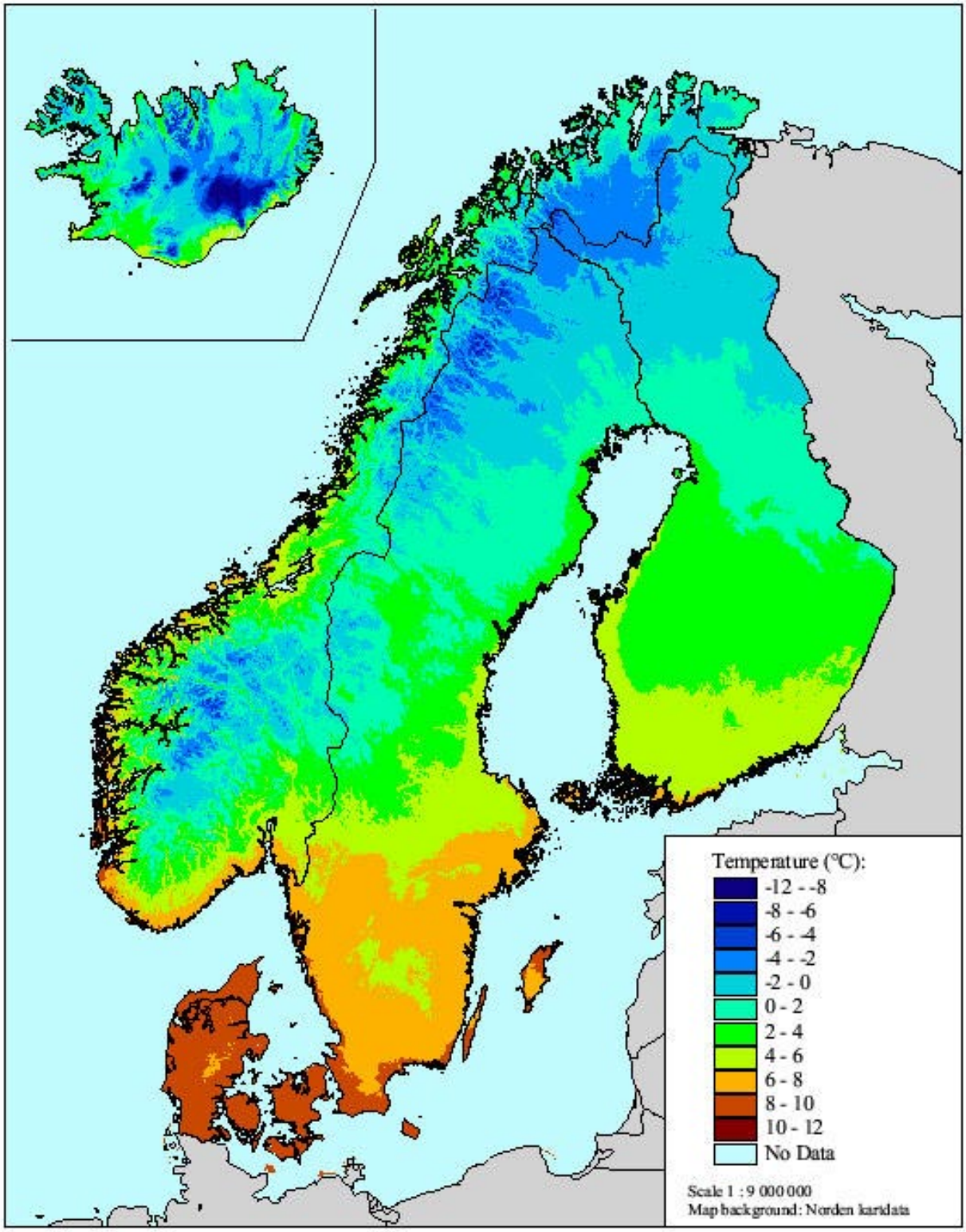

Mean annual temperature range 1961-90

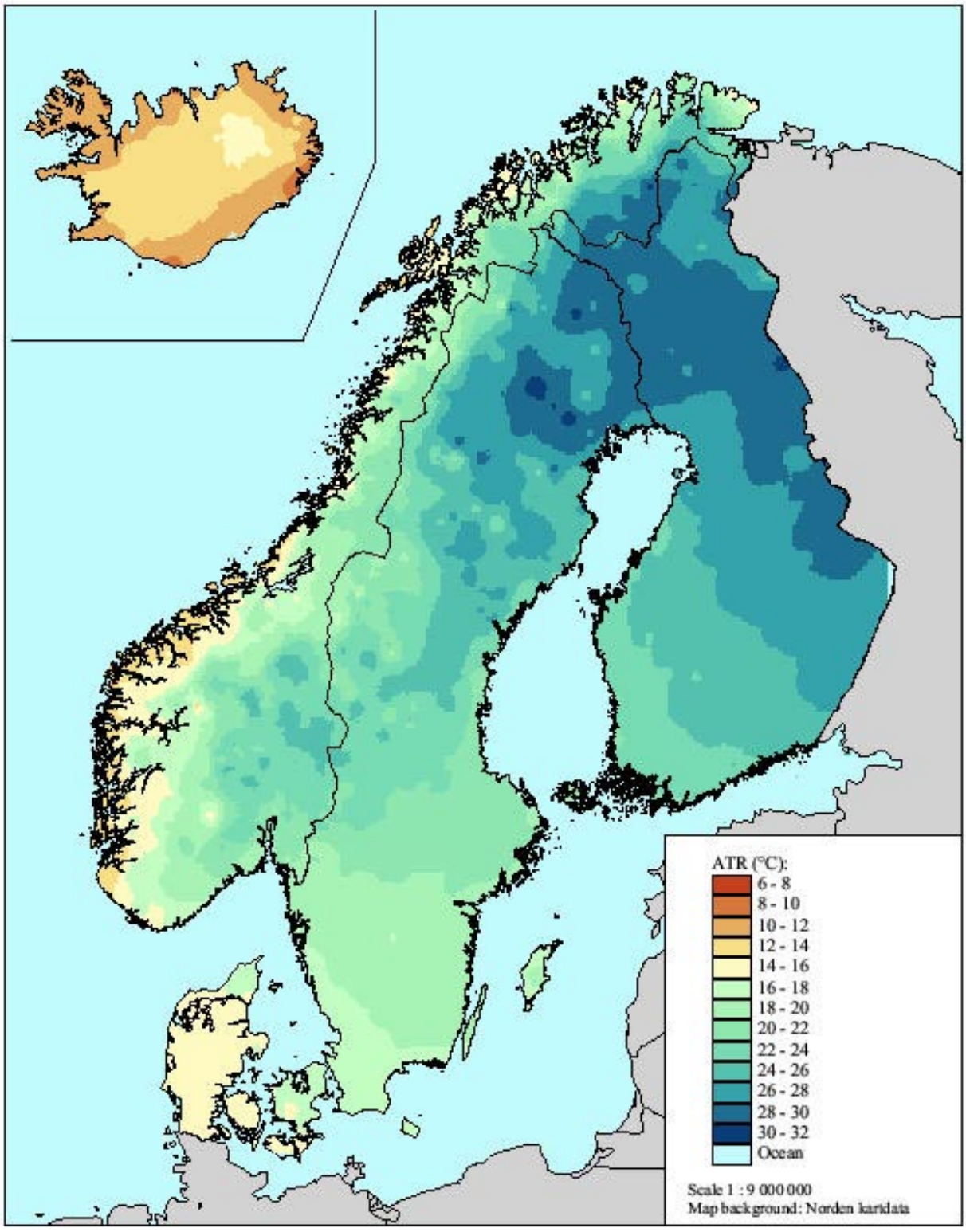

Longterm variability of temperature in the Nordic countries.

Figure 19 Temperature regions and location of selected stations.

Globally averaged, the annual mean temperatures at the end of the 20th century were more than 0.6 °C above those recorded at the end of the 19th century (WMO, 2000). Reconstructed temperatures for the Northern Hemisphere for the last 1000 years indicate that the 20th century was unusually warm, and that the 1990s probably was the warmest decade during the millennium as a whole.

The series presented by WMO (2000) show that the temperature increase both globally and in the Northern Hemisphere has mainly occurred in two periods, from ca.1900 to the 1930s and since the mid 1960s. Both globally and in the northern hemisphere, the present temperature level is substantially higher than in the 1930s. In the Northern Hemisphere north of 30N, the temperature level at the end of the 20th century is ca. 0.5 °C higher than in the 1930s.

The annual temperature has increased during the 20th century also in the Nordic region. The two periods of global warming are seen also in the Nordic region, but the magnitude and time evolution of the temperature is different in different parts of the region (Figure 20).

The temperature trends in Northern Europe during 1890-1990 were studied by Hanssen-Bauer et al (1996). More than 50 long-term temperature series were analysed by applying principal component analysis (PCA). By using a simple criteria concerning the influence of PCA's 1 and 2, the area was divided into "temperature regions". These regions are used as a basis for defining the 10 Nordic temperature regions shown in Figure 19. In each of these regions one representative, homogenised temperatures series was chosen. The locations of the selected stations are indicated in Figure 19.

In order to identify long-term trends and decadal scale variability in the selected temperature series, they were smoothed by two Gaussian low pass filters. The weighting coefficient in year j, G_j is given by:

$$G_j = \frac{\sum_{i=1}^{n} w_{ij} \cdot x_i}{\sum_{i=1}^{n} w_{ij}} \qquad w_{ij} = e^{\frac{-(i-j)^2}{2\sigma^2}} \qquad (1)$$

where the x_i is the original series which consists of n years, and σ is the standard deviation in the Gaussian distribution. For the analyses in the present chapter, filters with σ = 3 (Filter 1) and 9 (Filter 2) were chosen, which are favourable for studying variations on decal and 30-year time scales, respectively. The ends of filtered curves are very dependent on the first or last few values, which may influence the trends seriously.

Table 5. Linear trends (°C/decade) in annual temperature during 1890-1999

Station	Linear trend (°C/decade)
Svalbard Airport	+0.13
Karasjok	+0.02
Stykkisholmur	+0.05
Stensele	+0.08
Torshavn	+0.05
Helsinki	+0.10
Kjøremsgrendi	+0.05
Växjö	+0.03
Utsira	+0.05
Tranebjerg	+0.07

Figure 20 shows that in the southern part of the Nordic region, the present **annual** temperature level is the highest recorded during the last centennial. In the western (Faeroe Islands, Iceland) and northern (Svalbard, Karasjok) part, the temperature level during the 1930s was higher than the present level, both on a decadal (Filter 1) and long-term (Filter 2) basis. At the north-western stations (Svalbard Airport, Stykkisholmur and Torshavn) even the temperature level around 1960 was higher than at present. The linear trends (Table 5) show that during the period 1890-1999 the increase in temperatures in the Fennoscandian series varies between 0.02 °C/decade (Karasjok) to 0.10 °C/decade (Helsinki). At Svalbard Airport the linear increase during 1912-1999 is 0.13 °C/decade.

At the northern stations, the **winter** temperatures were higher in the 1930s than at present (at Svalbard Airport even 2-3 °C higher) (Figure 21). At the southern stations however, the present level is considerably higher than in the rest of the series. For most of the stations the lowest winter minima are found in the beginning of the series. Secondary minima are found in the 1960s and around 1980.

At several stations (e.g. Svalbard Airport, Stensele, Helsinki, Kjøremsgrendi, Utsira) the **spring** temperatures have increased steadily throughout the 20th century. Most stations experienced low spring temperatures in the beginning of the century, and rather high temperatures around 1950.

The **summer** temperatures were high over the whole region in the 1930s. At most stations both the filters 1 and 2 are indicating absolute maxima in that decade. The lowest summer temperatures were experienced in the early 1920s.

The **autumn** temperatures have increased during the last century, but at most stations the highest level (both filter 1 and 2) occurred in the middle of the century. Most stations experienced low autumn temperatures in the 1920s.

By studying the seasonal values, it is evident that the high annual temperatures in the 1930s were caused by warm autumns, winters and summers, while the high temperatures in the 1990s are caused by warm winters and springs. The reason why the annual temperatures generally are lower in the beginning of the series than in the 1960s and 1980s is not a lack of cold winters, but rather that the other seasons (especially the spring) usually are warmer during these later decades.

Hanssen-Bauer and Førland (2000) showed that for southern and north-western parts of Norway, the variation in atmospheric circulation over northern Europe can explain most of the observed trends and decadal scale variability in temperature since 1940. However, the positive trend in the annual mean temperature all over Norway during 1900-1940 was not modelled successfully using sea level pressure as the only predictor. Hanssen-Bauer and Førland (op.cit.) concluded that the variation in temperature in Norway during 1900-1940 probably is connected to changes in external forcing and/or atmosphere-ocean interactions.

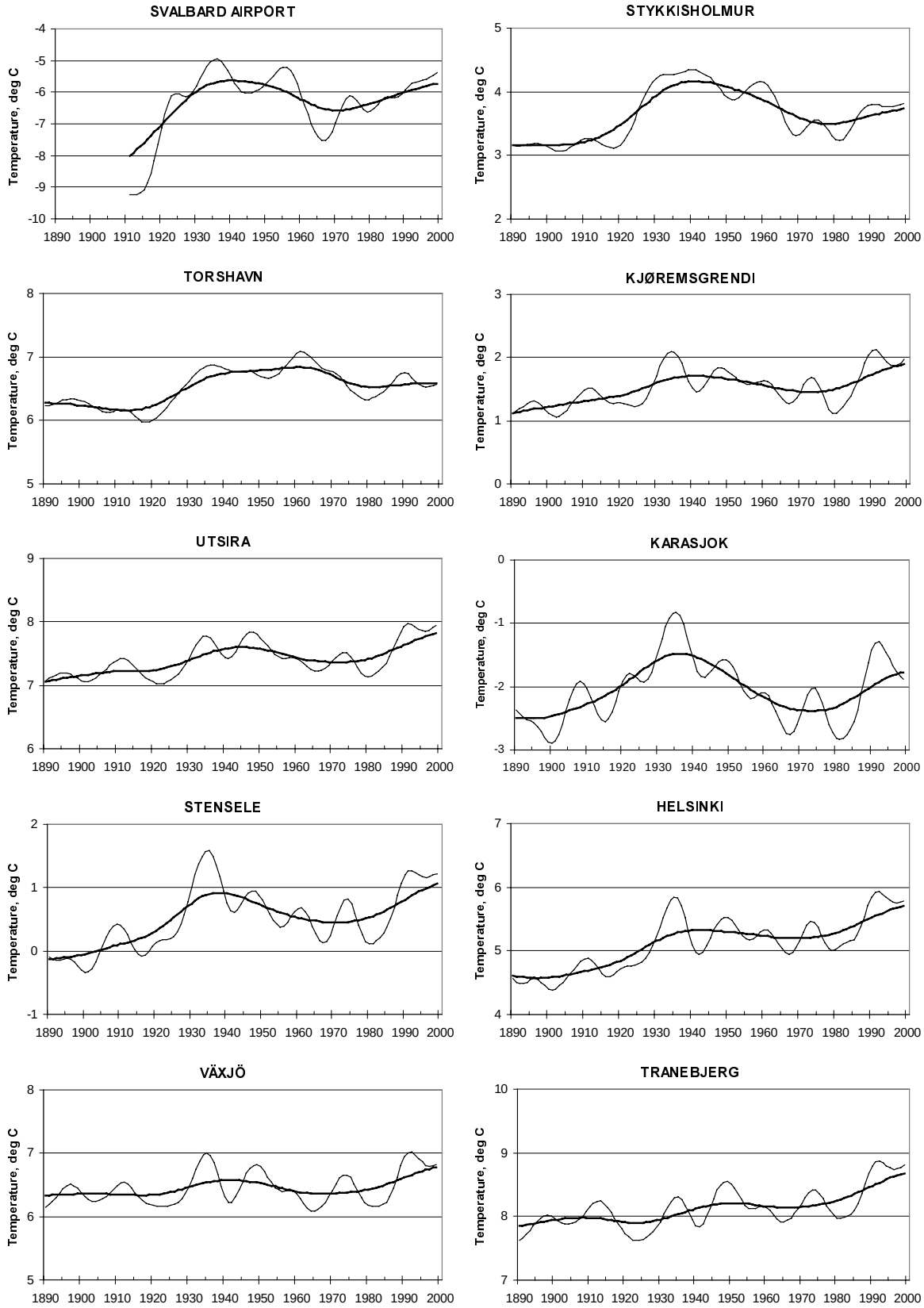

Figure 20. Low-pass filtered series of temperature for selected stations in the Nordic region.

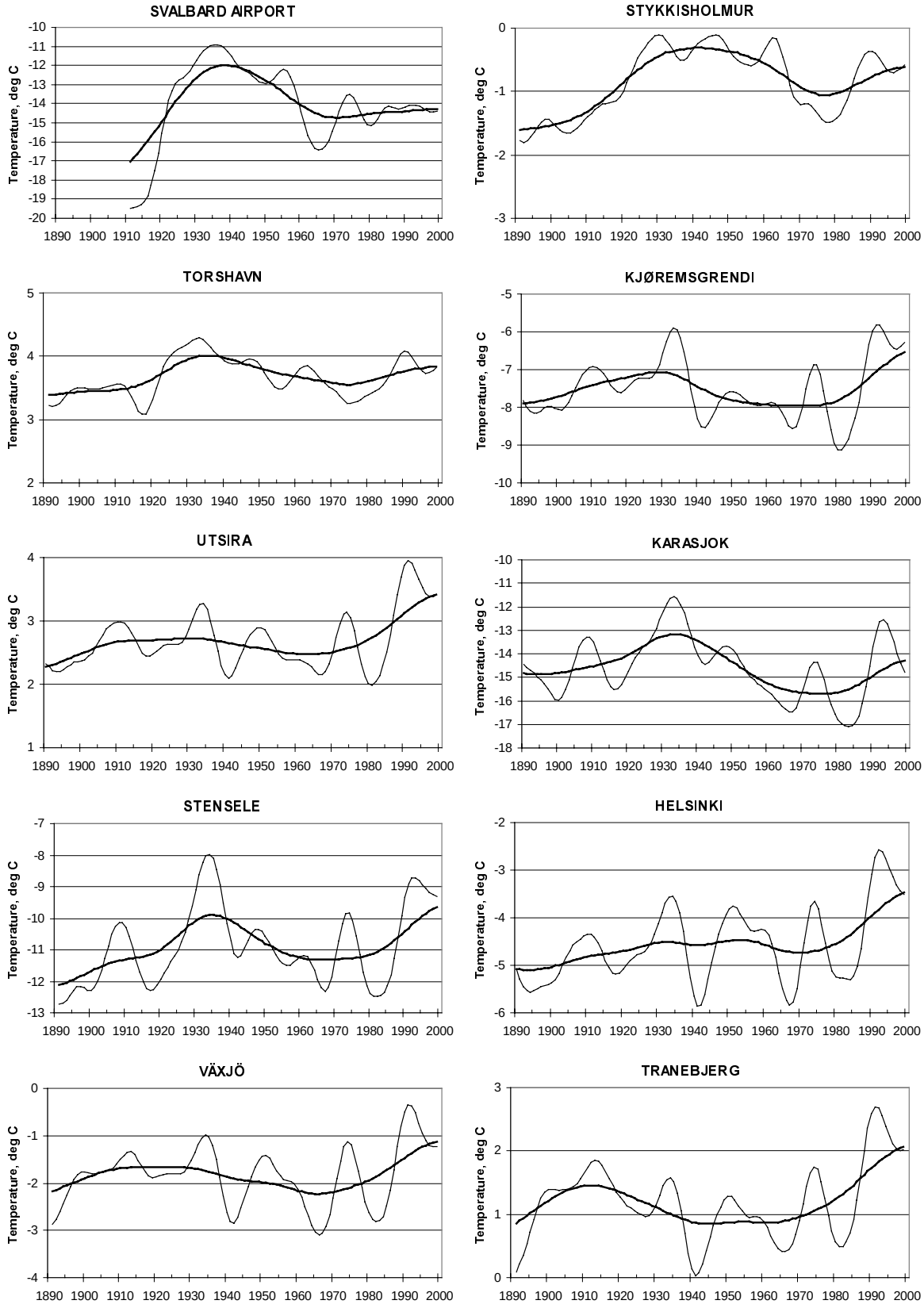

Figure 21. Low-pass filtered series of temperature for selected stations in the Nordic region.

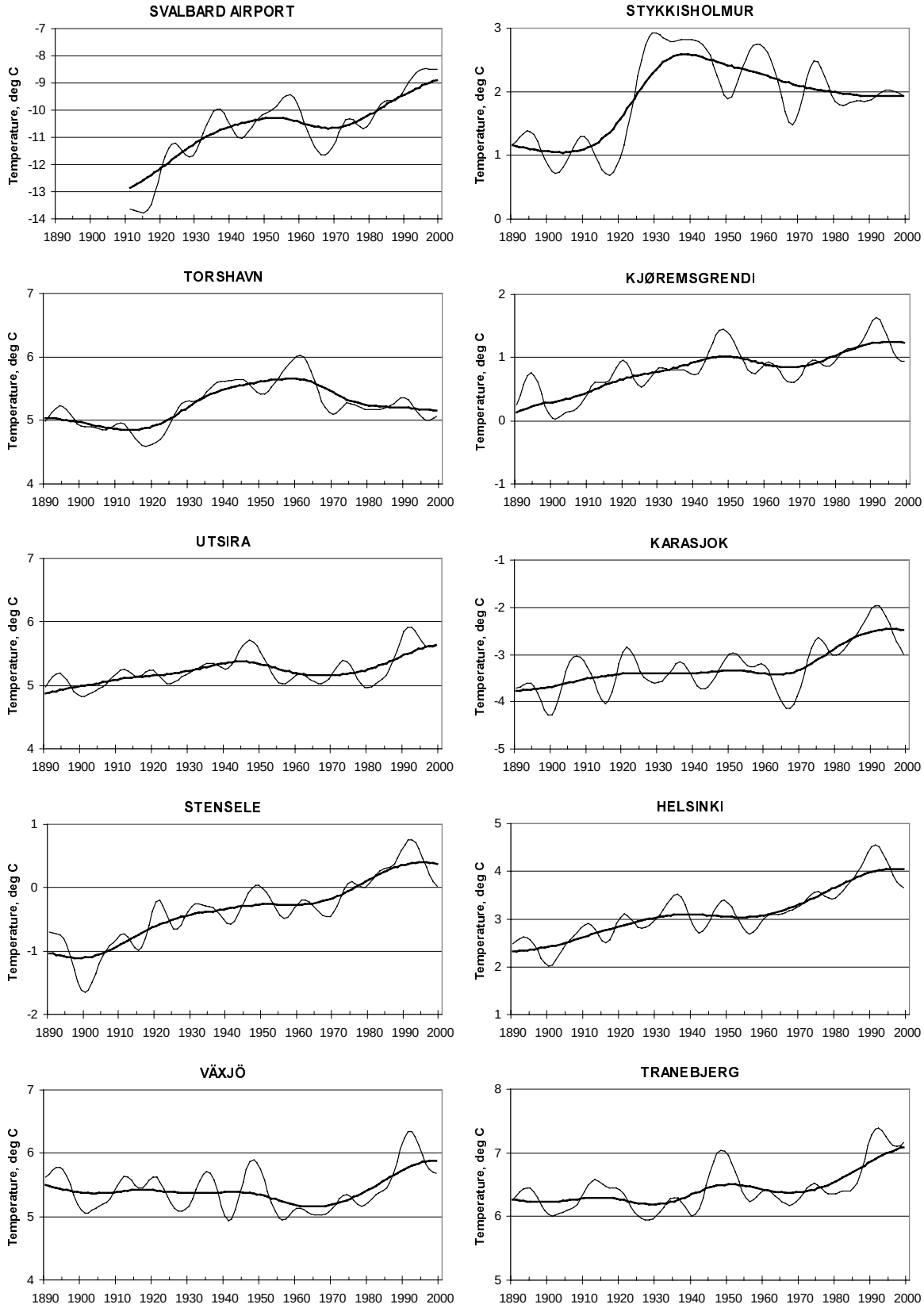

Figure 22. Low-pass filtered series of temperature for selected stations in the Nordic region.

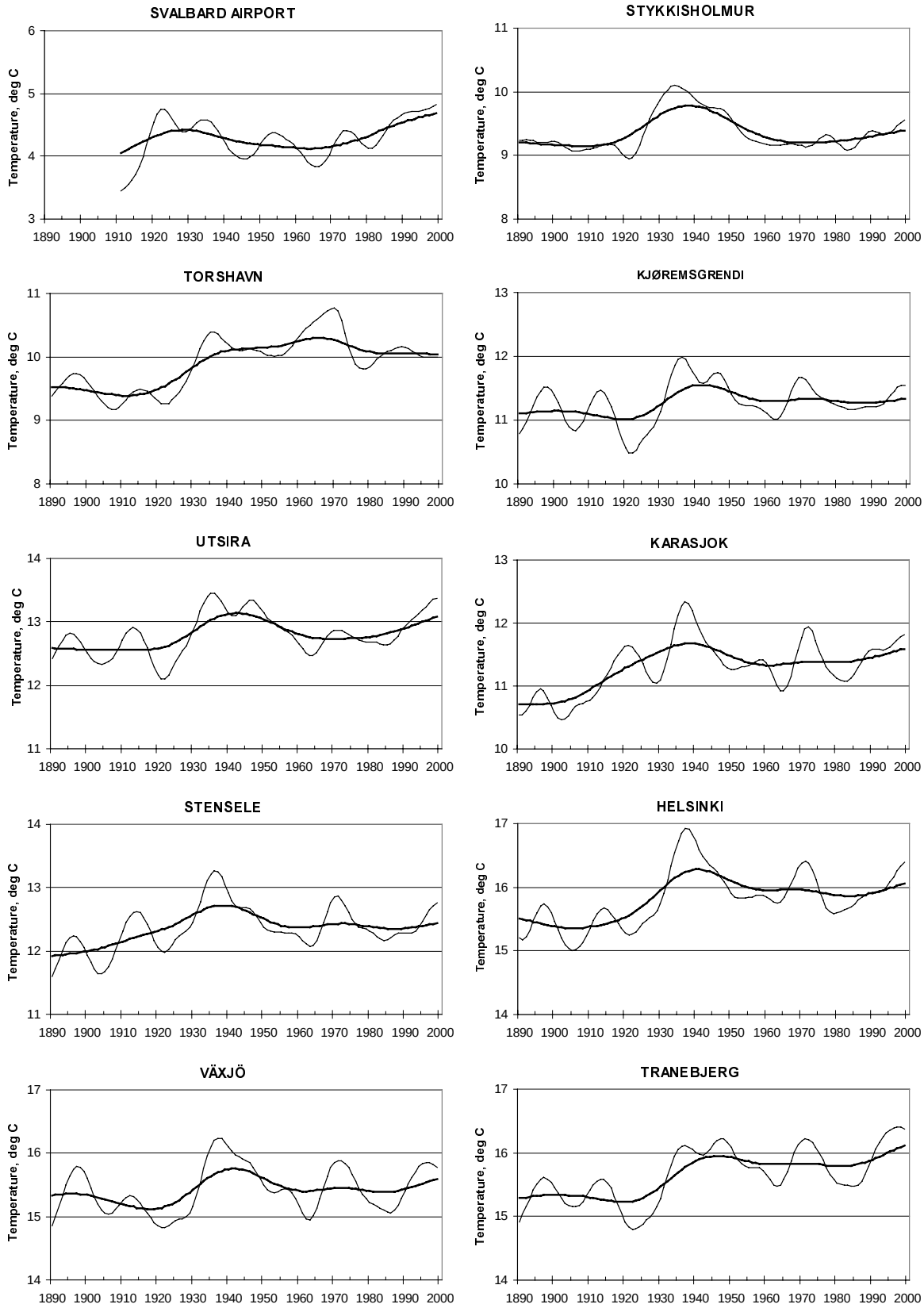

Figure 23. Low-pass filtered series of temperature for selected stations in the Nordic region.

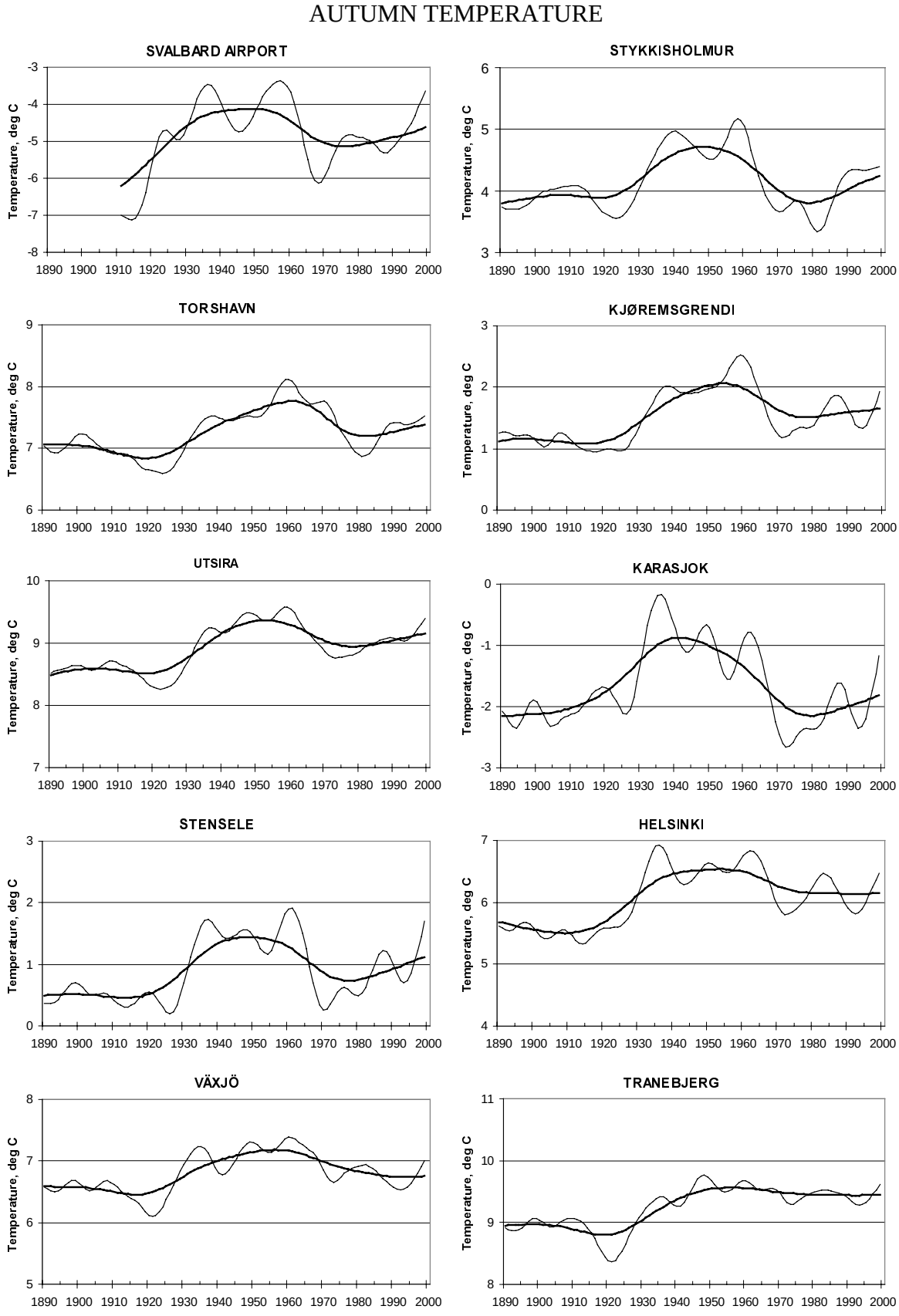

Figure 24. Low-pass filtered series of temperature for selected stations in the Nordic region.

Discussion & conclusions

This report presents maps of mean monthly temperatures for the period 1961-90. The spatial distributions of monthly temperatures are estimated by using the detrended kriging technique. Verification of the results shows that this method is able to reproduce the observed temperatures very well.

One problem by applying objective methods within climatology, is that the analysis is purely based on the observations. Thereby the method is not strictly valid outside the observation spectre. In this specific analysis the station network is biased. Most stations are located in populated areas at lower altitudes. This means that the characteristics in mountain areas are poorly described, or even not described at all in certain areas. In mountainous areas in the Nordic region, most stations are located in valleys. Because of frequent inversions in these valleys, and difficulties in assessing the vertical lapse rate, the temperatures in the mountain regions are probably estimated too low for the winter season.
The annual map is the mean of the twelve monthly maps. Similarly the seasonal maps are constructed as the mean of three monthly maps. By using this GIS-procedure monthly, seasonal and annual maps are consistent. On the other hand, by using this procedure the errors in the maps are added.

The temperature maps presented in this report are the first for the Nordic region derived by applying such an objective and consistent approach. This study shows the importance of regarding both local and regional characteristics in description of the local climate. Some of the results obtained here are new (e.g. the consistent monthly-seasonal-annual maps, and the map of annual temperature range), showing the possibilities of applying GIS in climatological analysis. The combination of GIS and spatial statistics is a very powerful tool which can be used for many purposes within climatology, e.g. within quality control and in production of fine-scale gridded climate data.

The next challenge should be to utilize these results, and extend the method to be applied on daily data.

The study shows that the Nordic region has large variability in temperature, both in space and time. An examination of homogeneous temperature series indicates that the annual temperature has increased by 0.3-1.0°C in different parts of Fennoscandia during the 20th century. The long-term temperature series show distinct variations on a decadal scale, reflecting the large climatic variability at high latitudes.

References

Alalammi, P. (1987) Atlas of Finland - Climate, National Board of Survey, 32 pp.

Aune, B. (1993) Nasjonalatlas for Norge, kartblad 3.1.6 (National atlas of Norway, map 3.1.6; in Norwegian), Statens Kartverk

Bruun, I. (1957) Lufttemperaturen i Norge, del I (The air temperature in Norway Vol. I; in Norwegian), Norwegian meteorological institute, 288 pp.

Cressie, N.O.A. (1991) Spatial statistics, Wiley & Son

Eliassen, A. and K.Pedersen (1977) Meterology, an introductory course. Vol. II Application to weather and weather systems, Universitetsforlaget (Scandinavian University Books)

Foltescu, D. and V.Foltescu (2000) Climate Applications based on High Resolution Datasets produced by the MESAN System, DNMI Report 08/00 KLIMA

Førland, E,J (1984) Lokalklima på Vestlandskysten (Local climate in Western Norway), Klima 6, pp. 22-36

Førland, E.J., A.van Engelen, I.Hanssen-Bauer,I., R.Heino, J.Ashcroft, B.Dahlström, G.Demarée, P.Frich, T.Jónsson, M.Mietus, G.Müller-Westermeier, T.Pálsdottir, H.Tuomenvirta and H.Vedin (1996) Changes in "normal" precipitation in the north Atlantic region, DNMI Report 7/96 KLIMA

Førland, E.J., B.Dahlström, R.Heino, T.Jónsson and H.Madsen (1998) NORDKLIM: Nordic Co-operation within climate activities. Project proposal of February 1999, 12 pp.

Hanssen-Bauer, I., (1999) Downscaling of temperature and precipitation in Norway based upon multiple regression of the principal components of the SLP field. DNMI-Report 21/99 KLIMA, 40pp.

Hanssen-Bauer, I. and E.J.Førland (2000) Temperature and precipitation variations in Norway and their links to atmospheric circulation. Accepted by Int.J. Climatol.

Hanssen-Bauer, I., P.Ø.Nordli and E.J.Førland (1996), Principal component analysis of the NACD temperature series, DNMI Report 1/96 KLIMA

Houghton, D.R. (1985) Handbook of applied meteorology, J.Wiley & Sons, 1461 pp.

Machenhauer, B., M.Windelband, M.Botzet, J.H.Christensen, M.Déqué, R.G.Jones, P.M.Ruti and G.Visconti (1998) Validation and analysis of regional present-day climate and climate change simulations over Europe. MPI Rep.275, Max-Planck Institüt für Meteorlogie, 80pp.

Prudhomme, C. and D.Reed (1999) Mapping extreme rainfall in a mountainous region using geostatistical techniques: A case study in Scotland, Int.J.Climatol. 19, pp. 1337-1356.

Raab,B. and H.Vedin (1995) Klimat, sjöar och vattendrag (Climate, Lakes and Rivers; in Swedish), SNA

Tveito, O.E. and E.J.Førland (1999) Mapping temperatures in Norway applying terrain information, geostatistics and GIS, Norsk geogr.tidsskrift 53 (4), pp. 202-212

USGS, (1996) GTOPO30 - Global topographic data, USGS Eros Data Centre, http://edcdaac.usgs.gov/gtopo30/gtopo30.html

WMO (1989) Calculation of mothly and annual 30-year standard normals, WCDP-No.10 (WMO-TD/No.341), Geneva, 11pp.

WMO (2000) WMO Statement on the Status of the Global Climate in 1999. World Meteorological Organisation, WMO-No. 913

Zheng, X. and R.E Basher (1996) Spatial modelling of New Zealand temperature normals, Int.J.Climatol, 16, pp. 307-319